Zweifler Laura (Orcid ID: 0000-0002-5696-4648)

# Anabolic actions of PTH in murine models: Two decades of insights

Laura E. Zweifler[1], Amy J. Koh[1], Stephanie Daignault-Newton[2], Laurie K. McCauley[1,3]

[1]Department of Periodontics and Oral Medicine, University of Michigan School of Dentistry, 1011 North University Avenue, Ann Arbor, MI 48109

[2]Biostatistics Unit, University of Michigan School of Public Health, 1415 Washington Heights, Ann Arbor, MI 48109

[3]Department of Pathology, Medical School, University of Michigan, 1301 Catherine Street, Ann Arbor, MI 48109

**Running Title:** Anabolic PTH in murine models

Corresponding Author:

Dr. Laurie K. McCauley

1011 N University Avenue

Ann Arbor, MI 48109

mccauley@umich.edu



This is the author manuscript accepted for publication and has undergone full peer review but has not been through the copyediting, typesetting, pagination and proofreading process, which may lead to differences between this version and the Version of Record. Please cite this article as doi: 10.1002/jbmr.4389

**Disclosure Page**

Funding support: DE028455 (LEZ), DK053904, DE022327 (LKM), CA093900 (SDN)

Disclosure Summary: LKM – Amgen Stock

**Abstract**

Parathyroid hormone (PTH) is produced by the parathyroid glands in response to low serum calcium concentrations where it targets bones, kidneys, and indirectly, intestines. The N-terminus of PTH has been investigated for decades for its ability to stimulate bone formation when administered intermittently (iPTH) and is used clinically as an effective anabolic agent for the treatment of osteoporosis. Despite great interest in iPTH and its clinical use, the mechanisms of PTH action remain complicated and not fully defined. More than 70 gene targets in more than 90 murine models have been utilized to better understand PTH anabolic actions. Since murine studies utilized wildtype mice as positive controls, a variety of variables were analyzed to better understand the optimal conditions under which iPTH functions. The greatest responses to iPTH were in male mice, with treatment starting later than 12 weeks of age, a treatment duration lasting 5-6 weeks, and a PTH dose of 30-60 μg/kg/day. This comprehensive study also evaluated these genetic models relative to the bone formative actions with a primary focus on the trabecular compartment revealing trends in critical genes and gene families relevant for PTH anabolic actions. The summation of these data revealed the gene deletions with the greatest increase in trabecular bone volume in response to iPTH. These included PTH and 1-α-hydroxylase (*Pth;1α(OH)ase*, 62-fold), amphiregulin (*Areg*, 15.8-fold), and PTH related protein (*Pthrp*, 10.2-fold). The deletions with the greatest inhibition of the anabolic response include deletions of: proteoglycan 4 (*Prg4*, -9.7-fold), low-density lipoprotein receptor-related protein 6 (Lrp6, 1.3-fold), and low-density lipoprotein receptor-related protein 5 (*Lrp5*, -1.0-fold). Anabolic actions of iPTH were broadly affected via multiple and diverse genes. This data provides critical insight for future research and development, as well as application to human therapeutics.

**Key words:** PTH, genetic animal models, parathyroid related disorders, anabolic, bone anabolism

**Introduction**

Parathyroid hormone (PTH) has been approved by the FDA since 2002, when teriparatide, a 34 amino acid analog of PTH, was accepted for the treatment of osteoporosis. More recently a PTH related protein (PTHrP) analog was also approved for the treatment of osteoporosis under the name abaloparatide.[1] It is well accepted that intermittent PTH (iPTH) therapy is anabolic for bone, while continuous PTH exposure is catabolic. The anabolic actions of iPTH in bone have been observed in animal models since 1929 using cats and rats.[2-5] These results were recapitulated in human patients [6,7] which led to the approval of this anabolic agent for therapeutic purposes.

As an endogenous endocrine mediator, PTH is released when the parathyroid gland detects a decrease in serum calcium concentration. Circulating PTH then targets the kidney and bone to increase serum calcium levels.[5] The effects of PTH and PTHrP in bone are achieved by binding to its type 1 receptor (PTH1R, a G-protein coupled receptor with 7 transmembrane domains) on osteoblasts.[8,9] This stimulates the production of RANKL in osteoblasts and subsequent osteoclastogenesis.[10] Indirectly, there is an increase in osteoblast numbers and bone formation.[11]

PTH is essential for fetal development, with newborn PTH-deficient mice exhibiting reduced cartilage matrix mineralization and trabecular bone, due to fewer metaphyseal osteoblasts.[12] Adult PTH-null mice exhibit decreased serum calcium, decreased 1,25-dihydroxyvitamin $D_3$, and increased serum phosphate.[13] Trabecular bone volume is increased in the femurs, tibiae, and vertebrae of mutant mice, and the number and size of tibial osteoclasts are reduced. Furthermore, there is a decreased mineral apposition rate.

PTHrP-null mice exhibit an osteoporotic phenotype that can be recapitulated in mice with targeted deletion in osteoblasts (*Pthrp$^{f/f}$;cre$^{coll}$*).[14] This model is more specific to the local bone environment, in which iPTH treatment increased mineral apposition rate, bone volume, trabecular number, trabecular thickness, trabecular connectivity, and cortical thickness in long bones. This could be attributed to increased receptor availability without endogenous PTHrP or changes in receptor desensitization (i.e. increased number of receptors because there is not desensitization from PTHrP). In either case, it is likely that PTHrP can modulate the response to PTH via the PTH1R receptor.[14]

**Materials and Methods**

Data for this study was collected from publications that have administered anabolic doses of iPTH from 2001-2020. Papers were accessed by searching scholarly search engines, such as PubMed, through December 2020. A highly relevant and consistent outcome of trabecular bone volume per total volume was used as a key and focused measure to compare the anabolic response in experimental gene targeted mice to wildtype controls in published studies. The PTH-induced bone volume response was derived for both gene targeted and wildtype mice separately [(PTH – Veh)/PTH]. Then, the relative response was calculated as a fold change by dividing the gene targeted response by the wildtype response. A fold change of 1.0 indicates that there was no change in the anabolic response between wildtype and gene targeted mice. If the fold change was greater than 1.0, the mutant mice had a greater anabolic response than wildtype, while between 0 and 1.0 the mutant mice had a less anabolic response. A negative fold change indicates that the mutant response to iPTH was catabolic. In some studies, actual numerical data was provided, whereas in others, data was derived from graphic representation. When bone

volume was only depicted graphically, values were estimated by measurement with a ruler to derive the gene targeted response relative to wildtype. Studies that showed an anabolic response to PTH in wildtype controls were included whereas those that did not demonstrate an anabolic response in controls were excluded (there were very few studies that did not display an anabolic response).

Most commonly, hPTH(1-34) was administered, although there were a few studies as indicated when the PTH differed (i.e., hPTH(1-84) or derived from a different source). Doses ranged from 20-160 μg/kg/day, but was typically between 40-100 μg/kg/day as specified in Table 2. PTH was administered by injection daily, 7 days/week, unless noted differently. Treatment time was typically 2-6 weeks of iPTH. The models are grouped under categories largely according to functional analyses in the supplemental text, alphabetically in Table 2, and numerically by fold change in Fig. 3. By assimilating the literature that has used anabolic PTH in genetic mouse models, we gain a better understanding of key genetic pathways as well as the overall complexity of PTH actions in bone.

**Results**

**Actions of iPTH in wildtype mice**

Since gene targeted murine studies utilized wildtype mice as positive controls, a variety of variables were analyzed to better understand the optimal conditions under which iPTH functions. Trabecular bone volume was compiled and organized by different categories (Fig. 2, Table 1). The groups were stratified by: sex, bone site, days per week of treatment, age at start of treatment, duration of treatment, and dose of iPTH. Strain was also considered and is listed in Table 2, however the only strain that had a large enough sample size for consideration was

C57BL/6. Since the interest of this section is comparing different categories, we did not include strain in the analysis. Most of these groups had a significant, positive correlation between the control trabecular bone volume and the iPTH treated bone volume (Table 1). Exceptions included using both sexes, analyzing the vertebrae, and treating with 50-60 μg/kg/day of PTH. Although this does not suggest that those indices should not be used in future studies, caution should be taken if drawing conclusions based only on trabecular bone volume.

Correlation graphs of the reported trabecular bone volume in control versus iPTH mice are shown in Fig. 2 and are separated by the categories mentioned. In order to understand how the variables relate within a category, the data was modeled with a linear regression and the slopes and corresponding 95% confidence interval were compared. Groups that had a significant correlation are discussed in the supplemental material, but all of the data is presented. This data can be used to inform future study design and interpretation.

We hypothesized that if a mouse has a high baseline bone volume, there is less capacity to mount an anabolic response to iPTH. Similarly, if an animal has a low baseline bone volume, they would show a greater response to iPTH. Analysis of the graph in Fig. 2G supports this, with the control bone volume plotted against the fold change response to PTH. Although biases exist as only studies that showed an anabolic response in wildtype mice were included, statistics support an inverse exponential relationship between these variables. To confirm that the data had an exponential relationship, and not a linear one, we calculated the Akaike Information Criterion (AIC), a statistical predictor of error between two models. The AIC for the exponential model is 36.44 lower than the linear model indicating that the exponential equation more precisely describes the relationship between the two variables.

**Analysis of PTH anabolic actions in bone using gene targeted mice**

The mechanism of anabolic iPTH and its effect on the bone microenvironment has been studied for decades and numerous mechanisms have been proposed based on *in vitro* and *in vivo* models.[15-17] A wide variety of genetic mouse models have been employed to elucidate the actions of PTH in bone over the past twenty years (Fig. 1, Table 2). With modern technology facilitating unprecedented genetic manipulation, this comprehensive study compiles the evidence of iPTH actions in gene targeted murine models. Of note, an important limitation is that while some mutations are global, many are focused on a subset of cells, and dependent on effective cre drivers and appropriate promoter selection. Hence the anabolic actions of PTH may reflect the effectiveness of the model as well as the targeted gene. Specific genotypes are indicated in Table 2, and discussed in detail in the supplemental materials.

The supplemental materials include detailed text descriptions of the literature using iPTH in gene targeted mice, which are summarized alphabetically by gene in Table 2. The models studied can be stratified by the function of the gene, including receptor activation and signaling pathways; downstream mediators in the fibroblast growth factor (FGF) family, wingless-related integration site (Wnt) family, bone morphogenetic protein (BMP) family, insulin-like growth factor (IGF) and growth hormone (GH), epidermal growth factor (EGF) family; and cell regulatory factors including apoptotic, immunity, extracellular matrix (ECM), cytoskeletal, and calcium regulation. The summation of these data demonstrated the gene deletions with the greatest increase in response to iPTH. These included PTH and 1-α-hydroxylase (*Pth;1α(OH)ase*, 62-fold)[18], amphiregulin (*Areg*, 15.8-fold)[19], and PTH related protein (*Pthrp*, 10.2-fold)[14] (Table 2). The deletions with the greatest inhibition of the anabolic response include deletions of:

proteoglycan 4 (*Prg4*, -9.7-fold)[20], low-density lipoprotein receptor-related protein 6 (*Lrp6*, 1.3-fold)[21], and low-density lipoprotein receptor-related protein 5 (*Lrp5*, -1.0-fold)[22] (Table 2). Several notable genes demonstrated no alteration of the anabolic action of PTH including major histocompatibility complex II knockout mice (*Mhc II*)[23], bone sialoprotein (*Bsp*)[24], and histone deacetylase 4 (*Hdac4*).[25] The models with the most study were insulin-like growth factor-1 (*Igf-1*).[26-29]

By detailing comparisons between reported iPTH studies, we are able to assimilate the role of different genes in the anabolic response. For example, Table 2 shows that mice with mutations in insulin-like growth factor I (*Igf-1*) can range in their response to iPTH, with bone volume fold changes relative to control mice from -0.3 -fold to 2.1-fold.[26-30] There has been long-standing interest in this gene, as it was the first genetic model to be studied with iPTH in 2001 because of the increase in IGF-1 production from osteoblasts in response to PTH.[26] A detailed analysis in the supplemental material compares the study design, mouse genetics, and conclusions of each report. These studies support a necessary role of IGF-1 in the anabolic response, as well as downstream targets, such as insulin receptor substrate-1 (IRS-1).[31]

**Discussion**

When mice are administered anabolic doses of PTH, signaling cascades affect proliferation and development of osteoblasts. There are many protein interactions and regulatory factors involved in this process, and it is unsurprising that when they are disrupted, the anabolic response does not achieve its full potential. The purpose of this study was to further elucidate PTH mechanisms by collectively analyzing the extensive work performed using mouse models.

The anabolic response in wildtype mice was analyzed to understand baseline differences and influences. Of the variables analyzed, the greatest responses to iPTH were in male mice, with treatment starting later than 12 weeks of age, a treatment duration lasting 5-6 weeks, and a PTH dose of 30-60 μg/kg/day. This data should be used to inform future study design for efficient use of resources. For example, based on the correlation data, male and female mice should be analyzed separately when treated with iPTH.

Collectively, the data suggests that starting treatment at greater than 12 weeks of age yields the highest response to iPTH. Mice are considered mature adults at this stage, but peak bone mass is closer to 16-18 weeks. The murine skeleton continues to grow past sexual maturity (about 7 weeks), whereas the human skeleton does not. PTH is commonly prescribed in post-menopausal women, and this population would be more comparative to mice that are at least 12 months old. Of the more than 130 cohorts of mice studied, only one was in this age range.[32]

Administering PTH for at least 5 days per week is sufficient to yield an anabolic response. While it is well documented that while continuous PTH is catabolic, iPTH is anabolic [33], this analysis has focused on the anabolic studies. Frolik et al. used a rat model to determine that the pharmacokinetics of PTH(1-34) varies with differing treatment regimens.[34] They found giving the same 80 micrograms per kilogram of PTH in a single injection or via six injections over one hour resulted in an anabolic response. However, administering the same 80 micrograms per kilogram of PTH over six or eight hours produced a catabolic response. They associated the anabolic iPTH in a temporal manner with the rapid increase in serum calcium, followed by tapering.

Analyses for this examination focused on the tibiae, femurs, and vertebrae. Although studies analyzing calvariae are reported in Table 2, there were not enough to include in the

correlation analysis. In humans, bone mineral density in post-menopausal women that were randomly assigned to PTH or placebo showed a larger percent change in the lumbar spine than femoral neck.[7] Since the vertebrae did not have a significant correlation between control bone volume and iPTH treated bone volume, we did not compare that data to the tibia and femur. Of note, this is comparing different outcomes (bone volume for murine studies and bone mineral density for human), measured by different variables and in a quadrupedal versus a bipedal species.

Relative to specific genetic aberrations that may inform PTH mechanisms, several trends are apparent from this analysis of more than 90 gene targeted studies. Bone health and energy metabolism are linked formulating a vital area of research interest. Many clinical conditions are also linked to altered energy expenditure, as reviewed by Motyl et al.[35] Among these targeted murine models with the largest increases in anabolic response to iPTH were Ampkα1, Hif-1α, and Cox2. Ampkα1 regulates energy consumption in the cell, working to promote ATP conservation or expenditure depending on current conditions.[36] Mice lacking Ampkα1 have a low bone mass with an increased anabolic response to iPTH.[37] Hif-1α is referred to as the master regulator of hypoxia because it is an oxygen-sensitive subunit of the Hif-1 complex (with Hif-1β). When oxygen is not present, Hif-1α is stabilized and translocated to the nucleus to bind to hypoxia-response elements.[38] Cox2 has been identified as a hypoxia responsive gene in colorectal cancer.[39] Authors of the work with Cox2 and iPTH were interested in its role regulating prostaglandin production, but it is possible that part of the effect of deleting this gene is affected by changes in energy metabolism. When these genes are deleted, the responsiveness to iPTH in bone is enhanced. Since these genes are activated when the cell is under metabolic stress and their

actions limit the PTH response, it is conceivable that they allow the cell to work at the capacity allowed by current energy conditions, limited by oxygen concentrations.

Ampkα1 and Hif-1α both regulate autophagy.[40,41] PTH prevents osteoblast apoptosis, prolonging the life of these cells.[42] It is also possible that in the absence of these genes, cell survival is further enhanced, leading to an increased response to iPTH. A presentation at the American Society for Bone and Mineral Research Annual Meeting in 2019 further connected autophagy and PTH mechanisms.[43] Using mice that had autophagy-deficient osteoblasts (*Fip200*$^{flox/flox}$; Osx-cre), Qi et al. showed a blunted anabolic response. Taken together, the evidence supports a relationship between autophagy and iPTH.

Canonical Wnt signaling promotes osteoblast expansion and function. Soluble ligands bind to the receptors (including LRPs) that induce stabilization of β-cat, allowing it to translocate to the nucleus and alter gene expression.[44] In mice with mutations in Lrp6 and β-cat, there were similar anabolic responses to PTH (vertebrae and femur when β-cat deletion under control of DMP1, and in the vertebrae when under control of Osx). Other Wnt family member proteins have been studied with iPTH, and it is clear that this pathway is critical for its anabolic effects in bone. N-cadherin restrains Wnt signaling and bone formation in osteoblasts.[45] Interestingly, when the gene for N-cadherin, *Cdh2*, is disrupted, the anabolic response to iPTH is increased. When both positive and negative regulators of Wnts are affected, the response to iPTH increases, suggesting anabolic PTH is sensitive to slight changes in Wnts.

N-cadherin may affect PTH responsiveness through other mechanisms as well. Expression of *Cdh2* is increased with maturity of osteoblasts and decreased expression is associated with osteosarcoma.[46,47] N-cadherin mediates cell-to-cell adhesion, highlighting the effect of

interaction with the microenvironment on osteoblasts. Mdx mice have a mutation in dystrophin, a protein that also helps osteoblasts interact with their environment by connecting the cytoplasm to the extracellular matrix in a complex. Disruption in dystrophin function increases the anabolic response to iPTH. Both N-cadherin and dystrophin are affected by calcium. N-cadherin is a calcium dependent glycoprotein, while Mdx mice exhibit increased intracellular calcium levels.[48] It is possible that these changes in calcium regulation alter responsiveness to iPTH.

This paper summarizes decades of work aimed to outline the mechanisms of anabolic iPTH, with more studies surely forthcoming. The reports described highlight the importance of many cell types in the bone microenvironment. Signaling starts in the osteoblast, depends on intracellular second messengers, and is then affected by/affects microenvironmental cues and other organ systems formulating a complex and dynamic process that results in bone formation and bone accrual. The insights from the analysis of the pooled data provide better direction for future experiments and appropriate interpretation.

**Acknowledgements**

The authors would like to thank the Consulting for Statistics, Computing, and Analytics Research (CSCAR) team at the University of Michigan for their advice. We would also like to acknowledge the National Institute of Dental and Craniofacial Research (NIDCR, DE028455 to LEZ, DE022327 to LKM), the National Institute of Diabetes and Digestive and Kidney Diseases (NIDDK, DK053904 to LKM), and the National Cancer Institute (NCI, CA093900 to SDN) of the National Institutes of Health (NIH) for funding support.

Authors' roles: Study design: LEZ and LKM. Data collection: LEZ and AJK. Data analysis: LEZ, AJK and SDN. Data interpretation: LEZ, SDN, LKM. Drafting manuscript: LEZ. Revising

manuscript content: LEZ and LKM. Approving final version of manuscript: LEZ, AJK, SDN, and LKM. LKM takes responsibility for the integrity of the data analysis.

**References**


1. Shirley M. Abaloparatide: first global approval. Drugs. Aug 2017;77(12):1363-8.
2. Burrows RB. Variations produced in bones of growing rats by parathyroid extracts. Am J Anat. Jan 1938;62(2):237-90.
3. Pugsley LI. The effect of parathyroid hormone and of irradiated ergosterol on calcium and phosphorous metabolism in the rat. J Physiol. Nov 5 1932;76(3):315-28.
4. Pugsley LI, Selye H. The histological changes in the bone responsible for the action of parathyroid hormone on the calcium metabolism of the rat. J Physiol. Jul 28 1933;79(1):113-7.
5. Bauer W, Aub JC, Albright F. Studies of calcium and phosphorus metabolism : V. A study of the bone trabeculae as a readily available reserve supply of calcium. J Exp Med. Jan 1 1929;49(1):145-62.
6. Lindsay R, Nieves J, Formica C, Henneman E, Woelfert L, Shen V, et al. Randomised controlled study of effect of parathyroid hormone on vertebral-bone mass and fracture incidence among postmenopausal women on oestrogen with osteoporosis. Lancet. Aug 23 1997;350(9077):550-5.
7. Neer RM, Arnaud CD, Zanchetta JR, Prince R, Gaich GA, Reginster JY, et al. Effect of parathyroid hormone (1-34) on fractures and bone mineral density in postmenopausal women with osteoporosis. N Engl J Med. May 10 2001;344(19):1434-41.
8. Juppner H, Abou-Samra AB, Freeman M, Kong XF, Schipani E, Richards J, et al. A G protein-linked receptor for parathyroid hormone and parathyroid hormone-related peptide. Science. Nov 15 1991;254(5034):1024-6.
9. Datta NS, Abou-Samra AB. PTH and PTHrP signaling in osteoblasts. Cell Signal. Aug 2009;21(8):1245-54.
10. McSheehy PM, Chambers TJ. Osteoblast-like cells in the presence of parathyroid hormone release soluble factor that stimulates osteoclastic bone resorption. Endocrinology. Oct 1986;119(4):1654-9.
11. Jilka RL, O'Brien CA, Bartell SM, Weinstein RS, Manolagas SC. Continuous elevation of PTH increases the number of osteoblasts via both osteoclast-dependent and -independent mechanisms. J Bone Miner Res. Nov 2010;25(11):2427-37.
12. Miao D, He B, Karaplis AC, Goltzman D. Parathyroid hormone is essential for normal fetal bone formation. J Clin Invest. May 2002;109(9):1173-82.
13. Miao D, Li J, Xue Y, Su H, Karaplis AC, Goltzman D. Parathyroid hormone-related peptide is required for increased trabecular bone volume in parathyroid hormone-null mice. Endocrinology. Aug 2004;145(8):3554-62.
14. Miao D, He B, Jiang Y, Kobayashi T, Soroceanu MA, Zhao J, et al. Osteoblast-derived PTHrP is a potent endogenous bone anabolic agent that modifies the therapeutic efficacy of administered PTH 1-34. J Clin Invest. Sep 2005;115(9):2402-11.

15. Rodan GA, Martin TJ. Role of osteoblasts in hormonal control of bone resorption-a hypothesis. Calcif Tissue Int. 1981;33(4):349-51.
16. Jones SJ, Boyde A. Experimental study of changes in osteoblastic shape induced by calcitonin and parathyroid extract in an organ culture system. Cell Tissue Res. Jul 6 1976;169(4):499-65.
17. Parfitt AM. The actions of parathyroid hormone on bone: relation to bone remodeling and turnover, calcium homeostasis, and metabolic bone diseases. Part II. PTH and bone cells: bone turnover and plasma calcium regulation. Metabolism. Aug 1976;25(8):909-55.
18. Xue Y, Karaplis AC, Hendy GN, Goltzman D, Miao D. Genetic models show that parathyroid hormone and 1,25-dihydroxyvitamin D3 play distinct and synergistic roles in postnatal mineral ion homeostasis and skeletal development. Hum Mol Genet. Jun 1 2005;14(11):1515-28.
19. Jay FF, Vaidya M, Porada SM, Andrukhova O, Schneider MR, Erben RG. Amphiregulin lacks an essential role for the bone anabolic action of parathyroid hormone. Mol Cell Endocrinol. Dec 5 2015;417:158-65.
20. Novince CM, Michalski MN, Koh AJ, Sinder BP, Entezami P, Eber MR, et al. Proteoglycan 4: a dynamic regulator of skeletogenesis and parathyroid hormone skeletal anabolism. J Bone Miner Res. Jan 2012;27(1):11-25.
21. Li C, Xing Q, Yu B, Xie H, Wang W, Shi C, et al. Disruption of LRP6 in osteoblasts blunts the bone anabolic activity of PTH. J Bone Miner Res. Oct 2013;28(10):2094-108.
22. Iwaniec UT, Wronski TJ, Liu J, Rivera MF, Arzaga RR, Hansen G, et al. PTH stimulates bone formation in mice deficient in Lrp5. J Bone Miner Res. Mar 2007;22(3):394-402.
23. Terauchi M, Li JY, Bedi B, Baek KH, Tawfeek H, Galley S, et al. T lymphocytes amplify the anabolic activity of parathyroid hormone through Wnt10b signaling. Cell Metab. Sep 2009;10(3):229-40.
24. Bouleftour W, Bouet G, Granito RN, Thomas M, Linossier MT, Vanden-Bossche A, et al. Blocking the expression of both bone sialoprotein (BSP) and osteopontin (OPN) impairs the anabolic action of PTH in mouse calvaria bone. J Cell Physiol. Mar 2015;230(3):568-77.
25. Wein MN, Liang Y, Goransson O, Sundberg TB, Wang J, Williams EA, et al. SIKs control osteocyte responses to parathyroid hormone. Nat Commun. Oct 19 2016;7:13176.
26. Miyakoshi N, Kasukawa Y, Linkhart TA, Baylink DJ, Mohan S. Evidence that anabolic effects of PTH on bone require IGF-I in growing mice. Endocrinology. Oct 2001;142(10):4349-56.
27. Rosen CJ, Ackert-Bicknell C, Beamer WG, Nelson T, Adamo M, Cohen P, et al. Allelic differences in a quantitative trait locus affecting insulin-like growth factor-I impact skeletal acquisition and body composition. Pediatr Nephrol. Mar 2005;20(3):255-60.
28. Yakar S, Bouxsein ML, Canalis E, Sun H, Glatt V, Gundberg C, et al. The ternary IGF complex influences postnatal bone acquisition and the skeletal response to intermittent parathyroid hormone. J Endocrinol. May 2006;189(2):289-99.
29. Elis S, Courtland HW, Wu Y, Fritton JC, Sun H, Rosen CJ, et al. Elevated serum IGF-1 levels synergize PTH action on the skeleton only when the tissue IGF-1 axis is intact. J Bone Miner Res. Sep 2010;25(9):2051-8.

30. Wang Y, Menendez A, Fong C, ElAlieh HZ, Chang W, Bikle DD. Ephrin B2/EphB4 mediates the actions of IGF-I signaling in regulating endochondral bone formation. J Bone Miner Res. Aug 2014;29(8):1900-13.
31. Yamaguchi M, Ogata N, Shinoda Y, Akune T, Kamekura S, Terauchi Y, et al. Insulin receptor substrate-1 is required for bone anabolic function of parathyroid hormone in mice. Endocrinology. Jun 2005;146(6):2620-8.
32. Hanyu R, Wehbi VL, Hayata T, Moriya S, Feinstein TN, Ezura Y, et al. Anabolic action of parathyroid hormone regulated by the β2-adrenergic receptor. Proc Natl Acad Sci U S A. May 8 2012;109(19):7433-8.
33. Dobnig H, Turner RT. The effects of programmed administration of human parathyroid hormone fragment (1-34) on bone histomorphometry and serum chemistry in rats. Endocrinology. Nov 1997;138(11):4607-12.
34. Frolik CA, Black EC, Cain RL, Satterwhite JH, Brown-Augsburger PL, Sato M, et al. Anabolic and catabolic bone effects of human parathyroid hormone (1-34) are predicted by duration of hormone exposure. Bone. Sep 2003;33(3):372-9.
35. Motyl KJ, Guntur AR, Carvalho AL, Rosen CJ. Energy Metabolism of Bone. Toxicol Pathol. Oct 2017;45(7):887-93.
36. Hardie DG. AMP-activated protein kinase: an energy sensor that regulates all aspects of cell function. Genes Dev. Sep 15 2011;25(18):1895-908.
37. Jeyabalan J, Shah M, Viollet B, Roux JP, Chavassieux P, Korbonits M, et al. Mice lacking AMP-activated protein kinase α1 catalytic subunit have increased bone remodelling and modified skeletal responses to hormonal challenges induced by ovariectomy and intermittent PTH treatment. J Endocrinol. Sep 2012;214(3):349-58.
38. Jiang BH, Zheng JZ, Leung SW, Roe R, Semenza GL. Transactivation and inhibitory domains of hypoxia-inducible factor 1α. Modulation of transcriptional activity by oxygen tension. J Biol Chem. Aug 1 1997;272(31):19253-60.
39. Kaidi A, Qualtrough D, Williams AC, Paraskeva C. Direct transcriptional up-regulation of cyclooxygenase-2 by hypoxia-inducible factor (HIF)-1 promotes colorectal tumor cell survival and enhances HIF-1 transcriptional activity during hypoxia. Cancer Res. Jul 1 2006;66(13):6683-91.
40. Zhang H, Bosch-Marce M, Shimoda LA, Tan YS, Baek JH, Wesley JB, et al. Mitochondrial autophagy is an HIF-1-dependent adaptive metabolic response to hypoxia. J Biol Chem. Apr 18 2008;283(16):10892-903.
41. Kim J, Kundu M, Viollet B, Guan KL. AMPK and mTOR regulate autophagy through direct phosphorylation of Ulk1. Nat Cell Biol. Feb 2011;13(2):132-41.
42. Jilka RL, Weinstein RS, Bellido T, Roberson P, Parfitt AM, Manolagas SC. Increased bone formation by prevention of osteoblast apoptosis with parathyroid hormone. J Clin Invest. Aug 1999;104(4):439-46.
43. Qi SQ, Wang L, Choi HK, McCauley L, Liu F, Pan J, et al. Fip200, an essential autophagy gene, mediates the anabolic action of PTH in bone. J Bone Miner Res. Abstract Dec 2019;34(32):22-3.
44. Westendorf JJ, Kahler RA, Schroeder TM. Wnt signaling in osteoblasts and bone diseases. Gene. Oct 27 2004;341:19-39.

45. Hay E, Laplantine E, Geoffroy V, Frain M, Kohler T, Muller R, et al. N-cadherin interacts with axin and LRP5 to negatively regulate Wnt/β-catenin signaling, osteoblast function, and bone formation. Mol Cell Biol. Feb 2009;29(4):953-64.
46. Ferrari SL, Traianedes K, Thorne M, Lafage-Proust MH, Genever P, Cecchini MG, et al. A role for N-cadherin in the development of the differentiated osteoblastic phenotype. J Bone Miner Res. Feb 2000;15(2):198-208.
47. Marie PJ. Role of N-cadherin in bone formation. J Cell Physiol. Mar 2002;190(3):297-305.
48. Morgenroth VH, Hache LP, Clemens PR. Insights into bone health in Duchenne muscular dystrophy. Bonekey Rep. 2012;1:9.
49. Samadfam R, Xia Q, Miao D, Hendy GN, Goltzman D. Exogenous PTH and endogenous 1,25-dihydroxyvitamin D are complementary in inducing an anabolic effect on bone. J Bone Miner Res. Aug 2008;23(8):1257-66.
50. Yu S, Franceschi RT, Luo M, Fan J, Jiang D, Cao H, et al. Critical role of activating transcription factor 4 in the anabolic actions of parathyroid hormone in bone. PLoS One. Oct 23 2009;4(10):e7583.
51. Yamashita J, Datta NS, Chun YH, Yang DY, Carey AA, Kreider JM, et al. Role of Bcl2 in osteoclastogenesis and PTH anabolic actions in bone. J Bone Miner Res. May 2008;23(5):621-32.
52. Nagase Y, Iwasawa M, Akiyama T, Ogata N, Kadono Y, Nakamura M, et al. Antiapoptotic molecule Bcl-2 is essential for the anabolic activity of parathyroid hormone in bone. Ann N Y Acad Sci. Mar 2010;1192:330-7.
53. Ferrari SL, Pierroz DD, Glatt V, Goddard DS, Bianchi EN, Lin FT, et al. Bone response to intermittent parathyroid hormone is altered in mice null for β-arrestin2. Endocrinology. Apr 2005;146(4):1854-62.
54. Gesty-Palmer D, Flannery P, Yuan L, Corsino L, Spurney R, Lefkowitz RJ, et al. A β-arrestin-biased agonist of the parathyroid hormone receptor (PTH1R) promotes bone formation independent of G protein activation. Sci Transl Med. Oct 7 2009;1(1):1ra.
55. Kedlaya R, Kang KS, Hong JM, Bettagere V, Lim KE, Horan D, et al. Adult-onset deletion of β-catenin in (10kb) Dmp1-expressing cells prevents intermittent PTH-induced bone gain. Endocrinology. Aug 2016;157(8):3047-57.
56. Yu C, Xuan M, Zhang M, Yao Q, Zhang K, Zhang X, et al. Postnatal deletion of β-catenin in osterix-expressing cells is necessary for bone growth and intermittent PTH-induced bone gain. J Bone Miner Metab. Sep 2018;36(5):560-72.
57. Lu R, Wang Q, Han Y, Li J, Yang XJ, Miao D. Parathyroid hormone administration improves bone marrow microenvironment and partially rescues haematopoietic defects in Bmi1-null mice. PLoS One. 2014;9(4):e93864.
58. Khan MP, Khan K, Yadav PS, Singh AK, Nag A, Prasahar P, et al. BMP signaling is required for adult skeletal homeostasis and mediates bone anabolic action of parathyroid hormone. Bone. Nov 2016;92:132-44.
59. Cho SW, Soki FN, Koh AJ, Eber MR, Entezami P, Park SI, et al. Osteal macrophages support physiologic skeletal remodeling and anabolic actions of parathyroid hormone in bone. Proc Natl Acad Sci U S A. Jan 28 2014;111(4):1545-50.

60. Demiralp B, Chen HL, Koh AJ, Keller ET, McCauley LK. Anabolic actions of parathyroid hormone during bone growth are dependent on c-fos. Endocrinology. Oct 2002;143(10):4038-47.
61. Al-Dujaili SA, Koh AJ, Dang M, Mi X, Chang W, Ma PX, et al. Calcium sensing receptor function supports osteoblast survival and acts as a co-factor in PTH anabolic actions in bone. J Cell Biochem. Jul 2016;117(7):1556-67.
62. Robinson JW, Li JY, Walker LD, Tyagi AM, Reott MA, Yu M, et al. T cell-expressed CD40L potentiates the bone anabolic activity of intermittent PTH treatment. J Bone Miner Res. Apr 2015;30(4):695-705.
63. Revollo L, Kading J, Jeong SY, Li J, Salazar V, Mbalaviele G, et al. N-cadherin restrains PTH activation of Lrp6/ β-catenin signaling and osteoanabolic action. J Bone Miner Res. Feb 2015;30(2):274-85.
64. Yang H, Dong J, Xiong W, Fang Z, Guan H, Li F. N-cadherin restrains PTH repressive effects on sclerostin/SOST by regulating LRP6-PTH1R interaction. Ann N Y Acad Sci. Dec 2016;1385(1):41-52.
65. Takahashi A, Mulati M, Saito M, Numata H, Kobayashi Y, Ochi H, et al. Loss of cyclin-dependent kinase 1 impairs bone formation, but does not affect the bone-anabolic effects of parathyroid hormone. J Biol Chem. Dec 14 2018;293(50):19387-99.
66. Xu M, Choudhary S, Voznesensky O, Gao Q, Adams D, Diaz-Doran V, et al. Basal bone phenotype and increased anabolic responses to intermittent parathyroid hormone in healthy male COX-2 knockout mice. Bone. Aug 2010;47(2):341-52.
67. Liu F, Lee SK, Adams DJ, Gronowicz GA, Kream BE. CREM deficiency in mice alters the response of bone to intermittent parathyroid hormone treatment. Bone. Apr 2007;40(4):1135-43.
68. Pacheco-Costa R, Davis HM, Sorenson C, Hon MC, Hassan I, Reginato RD, et al. Defective cancellous bone structure and abnormal response to PTH in cortical bone of mice lacking Cx43 cytoplasmic C-terminus domain. Bone. Dec 2015;81:632-43.
69. Yao GQ, Wu JJ, Troiano N, Insogna K. Targeted overexpression of Dkk1 in osteoblasts reduces bone mass but does not impair the anabolic response to intermittent PTH treatment in mice. J Bone Miner Metab. Mar 2011;29(2):141-8.
70. Schneider MR, Dahlhoff M, Andrukhova O, Grill J, Glosmann M, Schuler C, et al. Normal epidermal growth factor receptor signaling is dispensable for bone anabolic effects of parathyroid hormone. Bone. Jan 2012;50(1):237-44.
71. Hurley MM, Okada Y, Xiao L, Tanaka Y, Ito M, Okimoto N, et al. Impaired bone anabolic response to parathyroid hormone in Fgf2-/- and Fgf2+/- mice. Biochem Biophys Res Commun. Mar 24 2006;341(4):989-94.
72. Xiao L, Fei Y, Hurley MM. FGF2 crosstalk with Wnt signaling in mediating the anabolic action of PTH on bone formation. Bone Rep. Dec 2018;9:136-44.
73. Yuan Q, Sato T, Densmore M, Saito H, Schuler C, Erben RG, et al. FGF-23/Klotho signaling is not essential for the phosphaturic and anabolic functions of PTH. J Bone Miner Res. Sep 2011;26(9):2026-35.
74. Xie Y, Yi L, Weng T, Huang J, Luo F, Jiang W, et al. Fibroblast growth factor receptor 3 deficiency does not impair the osteoanabolic action of parathyroid hormone on mice. Int J Biol Sci. 2016;12(8):990-9.

75. Chen H, Sun X, Yin L, Chen S, Zhu Y, Huang J, et al. PTH 1-34 ameliorates the osteopenia and delayed healing of stabilized tibia fracture in mice with achondroplasia resulting from gain-of-function mutation of FGFR3. Int J Biol Sci. 2017;13(10):1254-65.
76. Liu Z, Kennedy OD, Cardoso L, Basta-Pljakic J, Partridge NC, Schaffler MB, et al. DMP-1-mediated Ghr gene recombination compromises skeletal development and impairs skeletal response to intermittent PTH. FASEB J. Feb 2016;30(2):635-52.
77. Sun P, He L, Jia K, Yue Z, Li S, Jin Y, et al. Regulation of body length and bone mass by Gpr126/Adgrg6. Sci Adv. Mar 2020;6(12):eaaz0368.
78. Wang L, Quarles LD, Spurney RF. Unmasking the osteoinductive effects of a G-protein-coupled receptor (GPCR) kinase (GRK) inhibitor by treatment with PTH(1-34). J Bone Miner Res. Oct 2004;19(10):1661-70.
79. Sinha P, Aarnisalo P, Chubb R, Poulton IJ, Guo J, Nachtrab G, et al. Loss of Gsα in the Postnatal Skeleton Leads to Low Bone Mass and a Blunted Response to Anabolic Parathyroid Hormone Therapy. J Biol Chem. Jan 22 2016;291(4):1631-42.
80. Frey JL, Stonko DP, Faugere MC, Riddle RC. Hypoxia-inducible factor-1α restricts the anabolic actions of parathyroid hormone. Bone Res. 2014;2:14005.
81. Raggatt LJ, Qin L, Tamasi J, Jefcoat SC, Jr., Shimizu E, Selvamurugan N, et al. Interleukin-18 is regulated by parathyroid hormone and is required for its bone anabolic actions. J Biol Chem. Mar 14 2008;283(11):6790-8.
82. Cho SW, Pirih FQ, Koh AJ, Michalski M, Eber MR, Ritchie K, et al. The soluble interleukin-6 receptor is a mediator of hematopoietic and skeletal actions of parathyroid hormone. J Biol Chem. Mar 8 2013;288(10):6814-25.
83. Huang MS, Lu J, Ivanov Y, Sage AP, Tseng W, Demer LL, et al. Hyperlipidemia impairs osteoanabolic effects of PTH. J Bone Miner Res. Oct 2008;23(10):1672-9.
84. Li X, Garcia J, Lu J, Iriana S, Kalajzic I, Rowe D, et al. Roles of parathyroid hormone (PTH) receptor and reactive oxygen species in hyperlipidemia-induced PTH resistance in preosteoblasts. J Cell Biochem. Jan 2014;115(1):179-88.
85. Sawakami K, Robling AG, Ai M, Pitner ND, Liu D, Warden SJ, et al. The Wnt co-receptor LRP5 is essential for skeletal mechanotransduction but not for the anabolic bone response to parathyroid hormone treatment. J Biol Chem. Aug 18 2006;281(33):23698-711.
86. Li C, Wang W, Xie L, Luo X, Cao X, Wan M. Lipoprotein receptor-related protein 6 is required for parathyroid hormone-induced Sost suppression. Ann N Y Acad Sci. Jan 2016;1364:62-73.
87. Tamasi JA, Vasilov A, Shimizu E, Benton N, Johnson J, Bitel CL, et al. Monocyte chemoattractant protein-1 is a mediator of the anabolic action of parathyroid hormone on bone. J Bone Miner Res. Sep 2013;28(9):1975-86.
88. Gray SK, McGee-Lawrence ME, Sanders JL, Condon KW, Tsai CJ, Donahue SW. Black bear parathyroid hormone has greater anabolic effects on trabecular bone in dystrophin-deficient mice than in wild type mice. Bone. Sep 2012;51(3):578-85.
89. Michalski MN, Seydel AL, Siismets EM, Zweifler LE, Koh AJ, Sinder BP, et al. Inflammatory bone loss associated with MFG-E8 deficiency is rescued by teriparatide. FASEB J. Jul 2018;32(7):3730-41.

90. Hrdlicka HC, Pereira RC, Shin B, Yee SP, Deymier AC, Lee SK, et al. Inhibition of miR-29-3p isoforms via tough decoy suppresses osteoblast function in homeostasis but promotes intermittent parathyroid hormone-induced bone anabolism. Bone. Feb 2021;143:115779.
91. Mahalingam CD, Datta T, Patil RV, Kreider J, Bonfil RD, Kirkwood KL, et al. Mitogen-activated protein kinase phosphatase 1 regulates bone mass, osteoblast gene expression, and responsiveness to parathyroid hormone. J Endocrinol. Nov 2011;211(2):145-56.
92. Yu X, Milas J, Watanabe N, Rao N, Murthy S, Potter OL, et al. Neurofibromatosis type 1 gene haploinsufficiency reduces AP-1 gene expression without abrogating the anabolic effect of parathyroid hormone. Calcif Tissue Int. Mar 2006;78(3):162-70.
93. Robling AG, Childress P, Yu J, Cotte J, Heller A, Philip BK, et al. Nmp4/CIZ suppresses parathyroid hormone-induced increases in trabecular bone. J Cell Physiol. Jun 2009;219(3):734-43.
94. Childress P, Philip BK, Robling AG, Bruzzaniti A, Kacena MA, Bivi N, et al. Nmp4/CIZ suppresses the response of bone to anabolic parathyroid hormone by regulating both osteoblasts and osteoclasts. Calcif Tissue Int. Jul 2011;89(1):74-89.
95. He Y, Childress P, Hood M, Jr., Alvarez M, Kacena MA, Hanlon M, et al. Nmp4/CIZ suppresses the parathyroid hormone anabolic window by restricting mesenchymal stem cell and osteoprogenitor frequency. Stem Cells Dev. Feb 1 2013;22(3):492-500.
96. Machado do Reis L, Kessler CB, Adams DJ, Lorenzo J, Jorgetti V, Delany AM. Accentuated osteoclastic response to parathyroid hormone undermines bone mass acquisition in osteonectin-null mice. Bone. Aug 2008;43(2):264-73.
97. Kitahara K, Ishijima M, Rittling SR, Tsuji K, Kurosawa H, Nifuji A, et al. Osteopontin deficiency induces parathyroid hormone enhancement of cortical bone formation. Endocrinology. May 2003;144(5):2132-40.
98. Walker EC, Poulton IJ, McGregor NE, Ho PW, Allan EH, Quach JM, et al. Sustained RANKL response to parathyroid hormone in oncostatin M receptor-deficient osteoblasts converts anabolic treatment to a catabolic effect in vivo. J Bone Miner Res. Apr 2012;27(4):902-12.
99. Thouverey C, Caverzasio J. Suppression of p38α MAPK signaling in osteoblast lineage cells impairs bone anabolic action of parathyroid hormone. J Bone Miner Res. May 2016;31(5):985-93.
100. Clifton KB, Conover CA. Pregnancy-associated plasma protein-A modulates the anabolic effects of parathyroid hormone in mouse bone. Bone. Dec 2015;81:413-6.
101. Yorgan TA, Sari H, Rolvien T, Windhorst S, Failla AV, Kornak U, et al. Mice lacking plastin-3 display a specific defect of cortical bone acquisition. Bone. Jan 2020;130:115062.
102. Bonnet N, Conway SJ, Ferrari SL. Regulation of β catenin signaling and parathyroid hormone anabolic effects in bone by the matricellular protein periostin. Proc Natl Acad Sci U S A. Sep 11 2012;109(37):15048-53.
103. Xue Y, Zhang Z, Karaplis AC, Hendy GN, Goltzman D, Miao D. Exogenous PTH-related protein and PTH improve mineral and skeletal status in 25-hydroxyvitamin D-1α-hydroxylase and PTH double knockout mice. J Bone Miner Res. Oct 2005;20(10):1766-77.
104. Bedi B, Li JY, Tawfeek H, Baek KH, Adams J, Vangara SS, et al. Silencing of parathyroid hormone (PTH) receptor 1 in T cells blunts the bone anabolic activity of PTH. Proc Natl Acad Sci U S A. Mar 20 2012;109(12):E725-33.

105. Datta NS, Samra TA, Abou-Samra AB. Parathyroid hormone induces bone formation in phosphorylation-deficient PTHR1 knockin mice. Am J Physiol Endocrinol Metab. May 1 2012;302(10):E1183-8.
106. Saini V, Marengi DA, Barry KJ, Fulzele KS, Heiden E, Liu X, et al. Parathyroid hormone (PTH)/PTH-related peptide type 1 receptor (PPR) signaling in osteocytes regulates anabolic and catabolic skeletal responses to PTH. J Biol Chem. Jul 12 2013;288(28):20122-34.
107. Delgado-Calle J, Tu X, Pacheco-Costa R, McAndrews K, Edwards R, Pellegrini GG, et al. Control of bone anabolism in response to mechanical loading and PTH by distinct mechanisms downstream of the PTH receptor. J Bone Miner Res. Mar 2017;32(3):522-35.
108. Huck K, Sens C, Wuerfel C, Zoeller C, Nakchbandi IA. The Rho GTPase RAC1 in osteoblasts controls their function. Int J Mol Sci. Jan 8 2020;21(2).
109. Kawano T, Troiano N, Adams DJ, Wu JJ, Sun BH, Insogna K. The anabolic response to parathyroid hormone is augmented in Rac2 knockout mice. Endocrinology. Aug 2008;149(8):4009-15.
110. Philip BK, Childress PJ, Robling AG, Heller A, Nawroth PP, Bierhaus A, et al. RAGE supports parathyroid hormone-induced gains in femoral trabecular bone. Am J Physiol Endocrinol Metab. Mar 2010;298(3):E714-25.
111. Merciris D, Marty C, Collet C, de Vernejoul MC, Geoffroy V. Overexpression of the transcriptional factor Runx2 in osteoblasts abolishes the anabolic effect of parathyroid hormone in vivo. Am J Pathol. May 2007;170(5):1676-85.
112. Bodine PV, Seestaller-Wehr L, Kharode YP, Bex FJ, Komm BS. Bone anabolic effects of parathyroid hormone are blunted by deletion of the Wnt antagonist secreted frizzled-related protein-1. J Cell Physiol. Feb 2007;210(2):352-7.
113. Yao W, Cheng Z, Shahnazari M, Dai W, Johnson ML, Lane NE. Overexpression of secreted frizzled-related protein 1 inhibits bone formation and attenuates parathyroid hormone bone anabolic effects. J Bone Miner Res. Feb 2010;25(2):190-9.
114. Kramer I, Loots GG, Studer A, Keller H, Kneissel M. Parathyroid hormone (PTH)-induced bone gain is blunted in SOST overexpressing and deficient mice. J Bone Miner Res. Feb 2010;25(2):178-89.
115. Robling AG, Kedlaya R, Ellis SN, Childress PJ, Bidwell JP, Bellido T, et al. Anabolic and catabolic regimens of human parathyroid hormone 1-34 elicit bone- and envelope-specific attenuation of skeletal effects in Sost-deficient mice. Endocrinology. Aug 2011;152(8):2963-75.
116. Wu X, Pang L, Lei W, Lu W, Li J, Li Z, et al. Inhibition of Sca-1-positive skeletal stem cell recruitment by alendronate blunts the anabolic effects of parathyroid hormone on bone remodeling. Cell Stem Cell. Nov 5 2010;7(5):571-80.
117. Saito H, Gasser A, Bolamperti S, Maeda M, Matthies L, Jahn K, et al. TG-interacting factor 1 (Tgif1)-deficiency attenuates bone remodeling and blunts the anabolic response to parathyroid hormone. Nat Commun. Mar 22 2019;10(1):1354.
118. Merciris D, Schiltz C, Legoupil N, Marty-Morieux C, de Vernejoul MC, Geoffroy V. Over-expression of TIMP-1 in osteoblasts increases the anabolic response to PTH. Bone. Jan 2007;40(1):75-83.

119. Fowler TW, McKelvey KD, Akel NS, Vander Schilden J, Bacon AW, Bracey JW, et al. Low bone turnover and low BMD in Down syndrome: effect of intermittent PTH treatment. PLoS One. 2012;7(8):e42967.
120. Xiong L, Xia WF, Tang FL, Pan JX, Mei L, Xiong WC. Retromer in osteoblasts interacts with protein phosphatase 1 regulator subunit 14C, terminates parathyroid hormone's signaling, and promotes its catabolic response. EBioMedicine. Jul 2016;9:45-60.
121. Yorgan TA, Rolvien T, Sturznickel J, Vollersen N, Lange F, Zhao W, et al. Mice carrying a ubiquitous R235W mutation of Wnt1 display a bone-specific phenotype. J Bone Miner Res. Sep 2020;35(9):1726-37.

**Table and Figure Legends**

**Table 1. Statistical analysis of the trabecular bone response in wildtype mice.** Data was pooled to analyze Pearson's correlation of the trabecular response of wildtype mice to vehicle or iPTH. The $r^2$ and p-value are reported from this analysis. The slope and 95% confidence interval of the linear regression of the slope is also reported.

**Table 2. Genetic models treated with iPTH.** A summary of each publication using iPTH in a genetic model is alphabetized by target gene. The genotype, gender, PTH regimen, age of mice during treatment, bone site, fold change in trabecular bone volume per total volume (BV/TV) comparing targeted gene vs. WT (Targeted Gene/WT), number of osteoblasts per bone surface (N. Ob/BS), number of osteoclasts per bone surface (N. Oc/BS), strain, and year are listed.

**Fig 1.** Timeline of gene targeted mouse models of PTH anabolic actions in bone.

**Figure 2. Trabecular bone response in WT mice.** (A-F) Trabecular bone volume is graphed for vehicle-treated (X-axis) and PTH-treated (Y-axis) wildtype mice. Each plot stratifies a different variable, including (A) sex, (B) bone site analyzed, (C) days per week of PTH treatment, (D) age at

the start of treatment, (E) duration of treatment, or (F) dose of treatment. Linear regression of the slope was analyzed for each group and compared within a variable, and the p-value is reported. (G) Control trabecular bone volume in wildtype mice and the fold change of trabecular bone volume in response to PTH in wildtype mice is plotted. The Akaike Information Criterion (AIC) is a statistical predictor of error between two models, and was used to confirm an inverse exponential relationship between control bone volume and the fold change in bone volume with PTH in wildtype mice.

**Figure 3. Fold change (FC) of PTH-/control-treated trabecular bone volume per total volume per targeted gene model.** The response to PTH treatment in gene targeted murine models was calculated using the bone volume fold change in mutant mice relative to the fold change of control treated mice. The X-axis lists the targeted gene. Some genes are listed multiple times, each of which represents a different study or cohort of animals listed in table 2. If there was no change between control and genetically modified treated animals, the fold change is 1, indicated by the marked line.

**Table 1**

| Category | Pearson's Correlation | | Linear Regression of the Slope | |
|---|---|---|---|---|
| **Gender** | **$r^2$** | **P-value** | **Slope** | **95% Confidence Interval** |
| Female (n=44) | 0.8990 | <0.0001 | 1.031 | 0.8746 to 1.1870 |
| Male (n=40) | 0.7698 | <0.0001 | 1.808 | 1.3160 to 2.3010 |
| Both (n=11) | 0.3470 | 0.2957 | 0.748 | -0.7763 to 2.2720 |
| **Bone Site** | **$r^2$** | **P-value** | **Slope** | **95% Confidence Interval** |
| Tibia (n=15) | 0.8631 | <0.0001 | 1.194 | 0.9090 to 1.4790 |
| Femur (n=63) | 0.5204 | <0.0001 | 1.690 | 1.2750 to 2.1050 |
| Vertebrae (n=21) | 0.1462 | 0.0872 | 0.620 | -0.0996 to 1.3400 |
| **Age at Start of Treatment** | **$r^2$** | **P-value** | **Slope** | **95% Confidence Interval** |
| 0-2 weeks (n=12) | 0.4261 | 0.0214 | 0.988 | 0.1802 to 1.7970 |
| 4-8 weeks (n=22) | 0.3150 | 0.0066 | 0.752 | 0.2348 to 1.2690 |
| 9-10 weeks (n=23) | 0.6942 | <0.0001 | 0.950 | 0.6640 to 1.2360 |
| 11-12 weeks (n=25) | 0.7071 | <0.0001 | 1.530 | 1.1050 to 1.9540 |

| | | | | |
|---|---|---|---|---|
| >12 weeks (n=22) | 0.6239 | <0.0001 | 2.031 | 1.2950 to 2.7670 |
| **Days per week of Treatment** | **$r^2$** | **P-value** | **Slope** | **95% Confidence Interval** |
| 5-5.5 (n=35) | 0.8758 | <0.0001 | 1.250 | 1.0060 to 1.4940 |
| 7 (n=66) | 0.6487 | <0.0001 | 1.3178 | 0.9320 to 1.7010 |
| **Duration of Treatment** | **$r^2$** | **P-value** | **Slope** | **95% Confidence Interval** |
| <4 weeks (n=23) | 0.6880 | <0.0001 | 1.347 | 0.9357 to 1.7590 |
| 4 weeks (n=48) | 0.3858 | <0.0001 | 0.885 | 0.5335 to 1.2016 |
| 5-6 weeks (n=22) | 0.6749 | <0.0001 | 2.459 | 1.6630 to 3.2550 |
| 7-12 weeks (n=12) | 0.6503 | 0.0015 | 0.790 | 0.3814 to 1.1970 |
| **Dose of Treatment (μg/kg/day)** | **$r^2$** | **P-value** | **Slope** | **95% Confidence Interval** |
| ≦30 (n=19) | 0.6201 | <0.0001 | 2.176 | 1.3050 to 3.0480 |
| 40 (n=19) | 0.6799 | <0.0001 | 1.565 | 1.0150 to 2.1140 |
| 50-60 (n=13) | 0.3717 | 0.0269 | 1.135 | 0.1559 to 2.1150 |
| 80 (n=44) | 0.4488 | <0.0001 | 0.919 | 0.6021 to 1.2370 |
| 90-160 (n=10) | 0.9454 | <0.0001 | 1.001 | 0.8050 to 1.1970 |

## Table 2

| Target Gene | Genotype | Gender | PTH Regimen | Age of Mice during Tx | Bone Site | FC in Trabecular BV/TV | N. Ob/BS | N. Oc/BS | Strain | Year | Ref. |
|---|---|---|---|---|---|---|---|---|---|---|---|
| 1α(OH)ase | *1α(OH)ase*$^{-/-}$ | ♂ | 40 μg/kg/day hPTH(1-34) | 12-16 weeks | Tibia | ~1.101 | No change | No change | C57BL/6J BALB/c | 2008 | (49) |
| Ampkα1 | *Ampkα1*$^{-/-}$ | NI | 80 μg/kg/day hPTH(1-34) (5 days/week) | 12-16 weeks | Tibia | ~4.250 | ND | ND | C57BL/6129/Sv | 2012 | (37) |
| Areg | *Areg*$^{-/-}$ | ♀ | 80 μg/kg/day hPTH(1-34) (5 days/week) | 12-16 weeks | Femur | ~15.75 | ND | Decreased | 129 C57BL/6 | 2015 | (19) |
| Atf4 | *Atf4*$^{-/-}$ | NI | 60 μg/kg/day hPTH(1-34) | 5-33 days | Femur | ~0.468 | ND | ND | Swiss Black | 2009 | (50) |
| Atf4 | *Atf4*$^{-/-}$ | NI | 60 μg/kg/day hPTH(1-34) | 5-33 days | Vertebrae | ~0.353 | ND | ND | Swiss Black | 2009 | (50) |
| Bcl2 | *Bcl2*$^{-/-}$ | NI | 50 μg/kg/day hPTH(1-34) | 4-13 days | Tibia | 1.054 | ND | ND | 129 C57BL/6 | 2009 | (51) |
| Bcl2 | *Bcl2*$^{-/-}$ *Bim*$^{+/-}$ | ♂ | 80 μg/kg/day hPTH(1-34) | 16-20 weeks | Tibia | ND | ND | No change | C57BL/6 (10$^{th}$ generation) | 2010 | (52) |
| β-arr2 | *β-arr2*$^{-/-}$ | ♂ | 80 μg/kg/day hPTH(1-34) (5 days/week) | 12-16 weeks | Femur | ND | Increased | Increased | C57Bl/6 | 2005 | (53) |
| β-arr2 | *β-arr2*$^{-/-}$ | ♂ | 80 μg/kg/day hPTH(1-34) (5 days/week) | 12-16 weeks | Vertebrae | ~0.000 | ND | ND | C57Bl/6 | 2005 | (53) |
| β-arr2 | *β-arr2*$^{-/-}$ | ♂ | 40 μg/kg/day hPTH(1-34) | 9-17 weeks | Vertebrae | ~0.428 | Decreased | Decreased | C57Bl/6 | 2009 | (54) |
| β-arr2 | *β-arr2*$^{-/-}$ | ♂ | 40 μg/kg/day hPTH(1-34) | 9-17 weeks | Tibia | ~0.179 | ND | ND | C57Bl/6 | 2009 | (54) |
| β-cat | *Dmp1-CreERt2;β-cat*$^{f/f}$ | ♂ | 30 μg/kg/day rhPTH(1-34) | 12.5-17.5 weeks | Femur | ~2.115 | ND | ND | C57Bl/6 129 | 2016 | (55) |
| β-cat | *Dmp1-CreERt2;β-cat*$^{f/f}$ | ♂ | 30 μg/kg/day rhPTH(1-34) | 12.5-17.5 weeks | Vertebrae | ~2.571 | ND | ND | C57Bl/6 129 | 2016 | (55) |
| β-cat | *Osx-Cre;β-cat*$^{f/f}$ | ♂ | 80 μg/kg/day rhPTH(1-34) | 7-11 weeks | Femur | ~1.120 | ND | ND | C57Bl/6 ((6$^{th}$ generation) | 2018 | (56) |
| β-cat | *Osx-Cre;β-cat*$^{f/f}$ | ♂ | 80 μg/kg/day rhPTH(1-34) | 7-11 weeks | Vertebrae | ~3.350 | ND | ND | C57Bl/6 (6$^{th}$ generation) | 2018 | (56) |
| $\beta_2$AR | *Adbr*$^{-/-}$ | ♀ | 80 μg/kg/day hPTH(1-34) (5 days/week) | 10-14 weeks | Femur | ~-0.081 | ND | Decreased | C57Bl/6 | 2012 | (32) |
| $\beta_2$AR | *Adbr*$^{-/-}$ | ♀ | 80 μg/kg/day hPTH(1-34) (5 days/week) | 10-14 weeks | Vertebrae | ~-0.131 | ND | ND | C57Bl/6 | 2012 | (32) |
| $\beta_2$AR | *Adbr*$^{-/-}$ | ♀ | 80 μg/kg/day hPTH(1-34) (5 days/week) | 54-58 weeks | Femur | ~-0.113 | ND | No change | C57Bl/6 | 2012 | (32) |
| BMI1 | *Bmi1*$^{-/-}$ | ♀♂ | 80 μg/kg/day hPTH(1-34) | 1-4 weeks | Femur | Cannot determine (missing necessary controls) | Cannot determine (missing | ND | 129Ola FVB/N hybrid | 2014 | (57) |

FC = fold change, NI = not indicated; ND = not determined; ~ = indicates that values are estimated from a graph, **=Bone area reported

| | | | | | | | | | | | |
|---|---|---|---|---|---|---|---|---|---|---|---|
| | | | | | | | necessary controls) | | | | |
| Bmp2, Bmp4 | *R26CreER/R26CreER and Bmp2$^{C/C}$. Bmp2$^{C/C}$; Bmp4$^{C/C}$; R26Cre$^{ER/+}$ (Bmp2/4 DCKO); OVX* | ♀ | 40 µg/kg/day hPTH(1-34) (5 days/week) | 10-12 - 16-18 weeks | Femur | Cannot determine (missing necessary controls) | ND | ND | NI | 2016 | (58) |
| BSP | *Bsp$^{-/-}$* | ♂ | 0.8 ug/uL PTH 1-84 (local injection) | 12-14 weeks | Calvaria | ~0.985 (BV reported) | ND | ND | 129 CD-1 | 2014 | (24) |
| C-FMS | *MAFIA* | ♀ | 50 µg/kg/day hPTH(1-34) | 16-22 weeks | Tibia | ~0.127 | ND | Decreased | C57Bl/6J | 2014 | (59) |
| C-FOS | *c-fos$^{-/-}$* | NI | 50 µg/kg/day hPTH(1-34) | 4-21 days | Vertebrae | ~0.316 | ND | ND | C57Bl/6 (5$^{th}$ generation) | 2002 | (60) |
| CaSR | *$^{Col\text{-}Bone}$CaSR$^{\Delta flox/\Delta flox}$* | NI | 50 µg/kg/day hPTH(1-34) | 4-17 days | Tibia | ~0.893 | ND | ND | C57Bl/6 CD-1 | 2015 | (61) |
| CD40L | *CD40L$^{-/-}$* | ♀ | 80 µg/kg/day hPTH(1-34) | 12-16 weeks | Femur | 0.135 | ND | Decreased | C57Bl/6 | 2014 | (62) |
| Cdh2 | *Osx-Cre::Cdh2$^{f/f}$* | ♂ | 80 µg/kg/day hPTH(1-34) (5 days/week) | 4 weeks of iPTH starting 12-16 weeks | Tibia | 3.815 | No change | Decreased | C57Bl/6 | 2014 | (63) |
| Cdh2 | *Dmp1-cre;Cdh2$^{f/f}$* | ♂ | 80 µg/kg/day hPTH(1-34) (5 days/week) | 8-12 weeks | Femur | 3.393 | Increased | Increased | C57Bl/6 | 2016 | (64) |
| Cdk1 | *Osx-Cre;Cdk1$^{f/f}$* | ♀ | 80 µg/kg/day hPTH(1-34) (5 days/week) | 12-16 weeks | Vertebrae | ~2.018 | Increased | No change | C57Bl/6129S6/SvEvTac | 2018 | (65) |
| Cox2 | *Cox2$^{-/-}$* | ♂ | 80 µg/kg/day hPTH(1-34) | 20-23 weeks | Femur | 1.669 | Increased | No change | CD-1 (9$^{th}$ generation) | 2010 | (66) |
| Cox2 | *Cox2$^{-/-}$* | ♂ | 80 µg/kg/day hPTH(1-34) | 20-23 weeks | Vertebrae | 5.688 | ND | ND | CD-1 (9$^{th}$ generation) | 2010 | (66) |
| Crem | *Crem$^{-/-}$* | ♂ | 160 µg/kg/day hPTH(1-34) | 10 days of iPTH from 11-12 weeks | Femur | ~0.312 | No change | Increased | 129Sv C57BL/6 | 2007 | (67) |
| Cx43 | *Cx43$^{\Delta CT/fl}$;DMP1-8kb-Cre* | ♀ | 100 µg/kg/day hPTH(1-34) | 16-18 wks | Femur | 1.154 | ND | ND | C57Bl/6 | 2015 | (68) |
| Dkk1 | *Dkk1 TG; 2.3-kb rat collagen type Ia promoter* | NI | 95 µg/kg/day hPTH(1-34) | 34 days of iPTH from 12-14 weeks | Tibia | ND | Decreased | Decreased | C57Bl/6 CD-1 | 2011 | (69) |
| Egdr | *Egfr$^{Wa5}$ (impaired EGFR signaling)* | ♀ | 80 µg/kg/day hPTH(1-34) (5 days/week) | 12-16 weeks | Femur | ~0.704** | ND | Decreased | C57Bl/6 | 2012 | (70) |
| Fgf2 | *Fgf2$^{-/-}$* | ♂ | 80 µg/kg/day hPTH(1-34) | 8-12 weeks | Femur | 0.647 | Decreased | No change | Black Swiss 129 Sv | 2006 | (71) |
| Fgf2 | *Fgf2$^{-/-}$* | ♀ | 80 µg/kg/day hPTH(1-34) | 60-64 weeks | Femur | 0.139 | ND | ND | Black Swiss 129 Sv | 2006 | (71) |

FC = fold change, NI = not indicated; ND = not determined; ~ = indicates that values are estimated from a graph, **=Bone area reported

| | | | | | | | | | | | |
|---|---|---|---|---|---|---|---|---|---|---|---|
| Fgf2 | *3.6Col1GFPsap h$^{tg/tg}$;Fgf2$^{-/-}$* | ♀ | 20 µg/kg/day PTH(1-34) | 12 weeks (8 hrs) | Tibia | ND | ND | ND | Black swiss 129Sv FVB/N | 2018 | (72) |
| Fgf23 | *Fgf23$^{-/-}$* | NI | 100 µg/kg/day hPTH(1-34) | 8-22 days | Femur | ~1.077 | No change | ND | C57Bl/6 129Sv | 2011 | (73) |
| Fgfr3 | *Fgfr3$^{-/-}$* | ♂ | 80 µg/kg/day hPTH(1-34) | 16-20 weeks | Femur | ~2.533 | Decreased | Increased | C3H | 2016 | (74) |
| Fgfr3 | *FGFR3$^{G369C/+}$* | NI | 80 µg/kg/day hPTH(1-34) | 8-12 weeks | Femur | ~2.814 | ND | ND | C57Bl/6 | 2017 | (75) |
| Ghr | *DMP1-Cre;GHR$^{f/f}$* | ♀ | 80 µg/kg/day hPTH(1-34) | 4-8 weeks | Femur | 0.234 | Decreased | No change | C57Bl/6 | 2015 | (76) |
| GPR126 | *Osx-cre;Gpr126$^{f/f}$* | ♀♂ | 80 µg/kg/day hPTH(1-34) | 5-30 days | Femur | ~1.975 | ND | ND | C57Bl/6 | 2020 | (77) |
| GRK2 | *GRK1$^{TG}$;1.3kb fragment of OG2 promoter* | ♀♂ | 40 µg/kg/day hPTH(1-34) | 36-40 weeks | Vertebrae | Cannot determine (missing necessary controls) | Increased | No change | B6SJLF1/J | 2009 | (78) |
| Gα$_s$ | *Gα$_s^{Osx-KO}$* | ♀♂ | 80 µg/kg/day hPTH(1-34) (5 days/week) | 8-12 weeks | Femur | 0.223 | Increased | Increased | C57Bl/6 CD1 | 2016 | (79) |
| HDAC4 | *HDAC4$^{fl/fl}$; DMP1-cre* | ♀ | 100 µg/kg/day hPTH(1-34) (5 days/week) | 8-12 weeks | NI | ~0.971 | ND | ND | C57Bl/6 | 2016 | (25) |
| HDAC4; HDAC5 | *HDAC5$^{-/-}$; HDAC4$^{fl/fl}$; DMP1-cre* | ♀ | 100 µg/kg/day hPTH(1-34) (5 days/week) | 8-12 weeks | NI | ~2.111 | ND | ND | C57Bl/6 | 2016 | (25) |
| HDAC5 | *HDAC5$^{-/-}$* | ♀ | 100 µg/kg/day hPTH(1-34) (5 days/week) | 8-12 weeks | NI | ~2.111 | ND | ND | C57Bl/6 | 2016 | (25) |
| Hif-1α | *Ocn-Cre;Hif-1αf/f* | ♀ | 20 µg/kg/day hPTH(1-34) | 10-16 weeks | Femur | ~1.511 | ND | ND | C57Bl/6 | 2014 | (80) |
| Hif-1α | *Ocn-Cre;Hif-1αf/f* | ♀ | 40 µg/kg/day hPTH(1-34) | 10-16 weeks | Femur | ~1.223 | ND | ND | C57Bl/6 | 2014 | (80) |
| Igf-1 | *Igf-1$^{-/-}$* | NI | 160 µg/kg/day hPTH(1-34) | 5-6.5 weeks | Femur | ND | ND | ND | NI | 2001 | (26) |
| Igf-1 | *B6.C3H-6T* | ♀ | 50 µg/kg/day hPTH(1-34) | 16-20 weeks | Femur | 0.704 | ND | ND | C57Bl/6 (10$^{th}$ generation) | 2005 | (27) |
| Igf-1 | *Igf1$^{fl/fl}$; Albumin-Cre* | ♂ | 50 µg/kg/day hPTH(1-34) (5 days/week) | 12-16 weeks | Vertebrae | ~2.150 | ND | ND | FVB/N, C57BL, and 129Sv | 2006 | (28) |
| Igf-1 | *ALS$^{-/-}$* | ♂ | 50 µg/kg/day hPTH(1-34) (5 days/week) | 12-16 weeks | Vertebrae | ~-0.300 | ND | ND | C57Bl/6 (6$^{th}$ generation) | 2006 | (28) |
| Igf-1 | *Igf1$^{fl/fl}$; Albumin-Cre; ALS$^{-/-}$* | ♂ | 50 µg/kg/day hPTH(1-34) (5 days/week) | 12-16 weeks | Vertebrae | ~-0.350 | ND | ND | FVB/N C57BL 129Sv | 2006 | (28) |
| Igf-1 | *HIT (hepatic IGF-1 transgene)* | ♂ | 50 µg/kg/day hPTH(1-34) | 12-16 weeks | Femur | ~1.622 | ND | ND | FVB/N | 2010 | (29) |
| Igf-1 | *HIT KO* | ♂ | 50 µg/kg/day hPTH(1-34) | 12-16 weeks | Femur | ~2.069 | ND | ND | FVB/N | 2010 | (29) |
| IGF-IR | *Ocn-Cre;Igf-IR$^{f/f}$* | NI | 80 µg/kg/day ratPTH(1-34) | 12-14 weeks | Tibia and Femur | ND | ND | ND | FVB/N | 2014 | (30) |

FC = fold change, NI = not indicated; ND = not determined; ~ = indicates that values are estimated from a graph, **=Bone area reported

| | | | | | | | | | | | |
|---|---|---|---|---|---|---|---|---|---|---|---|
| IL18 | *IL18*$^{-/-}$ | ♀ | 80 µg/kg/day hPTH(1-34) (5 days/week) | 4 weeks of iPTH starting at 7-8 weeks | Tibia and Femur | ND | ND | ND | DBA/1 | 2008 | (81) |
| IL6 | *IL6*$^{-/-}$ | ♀♂ | 50 µg/kg/day hPTH(1-34) | 3-24 days | Femur | ~0.596 | ND | Decreased | C57Bl/6 | 2013 | (82) |
| IL6 | *IL6*$^{-/-}$ | ♀♂ | 50 µg/kg/day hPTH(1-34) | 16-22 weeks | Femur | ~3.333 | ND | ND | C57Bl/6 | 2013 | (82) |
| Irs-1 | *Irs-1*$^{-/-}$ | ♂ | 80 µg/kg/day hPTH(1-34) | 10-14 weeks | Tibia and Femur | 0.090 | No change | Decreased | C57Bl6 CBA | 2005 | (31) |
| Irs-2 | *Irs-2*$^{-/-}$ | ♂ | 80 µg/kg/day hPTH(1-34) | 10-14 weeks | Tibia and Femur | 2.499 | Decreased | Decreased | C57Bl6 CBA | 2005 | (31) |
| Kl | *Kl*$^{-/-}$ | NI | 100 µg/kg/day hPTH(1-34) | 8-22 days | Femur | ~1.077 | No change | ND | C57Bl/6 129Sv | 2010 | (73) |
| Ldlr | *Ldlr*$^{-/-}$ | ♀ | 40 µg/kg/day hPTH(1-34) (5 days/week) | 20-25 weeks | Femur | 0.624 | Increased | Increased | C57Bl/6 | 2009 | (83) |
| Ldlr | *Ldlr*$^{-/-}$*; pOBCol3.6GFPtpz and pOBCol2.3GFP Cyan* | ♀ | 40 µg/kg/day hPTH(1-34) (5 days/week) | 5 weeks of iPTH starting at 8-12 weeks | Calveria | ND | Decreased | ND | C57Bl/6 | 2013 | (84) |
| Ldlr | *Ldlr*$^{-/-}$*; pOBCol3.6GFPtpz and pOBCol2.3GFP Cyan* | ♀ | 40 µg/kg/day hPTH(1-34) (5 days/week) | 5 weeks of iPTH starting at 8-12 weeks | Femur | ND | Decreased | ND | C57Bl/6 | 2013 | (84) |
| Lrp5 | *Lrp5*$^{-/-}$ | ♀♂ | 40 µg/kg/day hPTH(1-34) (5 days/week) | 12-16 weeks | Hindlimb | ND | ND | ND | 129S/J | 2006 | (85) |
| Lrp5 | *Lrp5*$^{-/-}$ | ♀ | 80 µg/kg/day hPTH(1-34) (every other day) | 20-26 weeks | Femur | ~0.435 | ND | ND | C57Bl/6 | 2009 | (22) |
| Lrp5 | *Lrp5*$^{-/-}$ | ♂ | 80 µg/kg/day hPTH(1-34) (every other day) | 20-26 weeks | Femur | ~-1.294 | ND | ND | C57Bl/6 | 2009 | (22) |
| Lrp5 | *Lrp5*$^{-/-}$ | ♀ | 80 µg/kg/day hPTH(1-34) (every other day) | 20-26 weeks | Vertebrae | ~10.000 | No change | No change | C57Bl/6 | 2009 | (22) |
| Lrp5 | *Lrp5*$^{-/-}$ | ♂ | 80 µg/kg/day hPTH(1-34) (every other day) | 20-26 weeks | Vertebrae | ~-1.028 | No change | No change | C57Bl/6 | 2009 | (22) |
| Lrp6 | *Ocn-cre;Lrp6*$^{f/f}$ | ♂ | 80 µg/kg/day hPTH(1-34) (5 days/week) | 8-12 weeks | Femur | ~-1.255 | Decreased | No change | C57Bl/6J 129 FVB/N | 2013 | (21) |
| Lrp6 | *Ocn-Cre;Lrp6*$^{f/f}$ | ♂ | 80 µg/kg/day hPTH(1-34) (5 days/week) | 8-12 weeks | Femur | ND | ND | ND | C57Bl/6J, 129 FVB/N | 2015 | (86) |
| MCP-1 | *Mcp-1*$^{-/-}$ | ♂ | 80 µg/kg/day hPTH(1-34) (5 days/week) | 16-22 weeks | Tibia | ~0.084 | ND | Decreased | C57Bl/6 | 2013 | (87) |
| MCP-1 | *Mcp-1*$^{-/-}$ | ♀♂ | 80 µg/kg/day hPTH(1-34) (5 days/week) | 20-26 weeks | ND | ND | ND | ND | C57Bl/6 | 2013 | (87) |
| Mdx | *C57BL/10ScSn/ DMD-mdx* | ♂ | 30 µg/kg/day black bearPTH(1-84) (5 days/week) | 4-10 weeks | Femur | ~5.833 | No change | Decreased | C57BL/610ScSn | 2012 | (88) |

FC = fold change, NI = not indicated; ND = not determined; ~ = indicates that values are estimated from a graph, **=Bone area reported

| | | | | | | | | | | | |
|---|---|---|---|---|---|---|---|---|---|---|---|
| Mfge8 | *Mfge8*$^{-/-}$ | ♀♂ | 50 µg/kg/day hPTH(1-34) | 16-22 weeks | Tibia | ~2.000 (reported as FC) | ND | Decreased | C57Bl/6 | 2018 | (89) |
| MHC I | *MHC I*$^{-/-}$ | NI | 80 µg/kg/day hPTH(1-34) | 5-9 weeks | Femur | ~0.173 | ND | ND | C57Bl/6 | 2009 | (23) |
| MHC I; MHC II | *MHC I*$^{-/-}$; *MHC II*$^{-/-}$ | NI | 80 µg/kg/day hPTH(1-34) | 5-9 weeks | Femur | ~0.058 | ND | ND | C57Bl/6 | 2009 | (23) |
| MHC II | *MHC II*$^{-/-}$ | NI | 80 µg/kg/day hPTH(1-34) | 5-9 weeks | Femur | ~1.038 | ND | ND | C57Bl/6 | 2009 | (23) |
| miR-29-3p | *miR-29-3p decoy* | ♀ | 80 µg/kg/day hPTH(1-34) (5 days/week) | 12-16 weeks | Femur | ~8.858 | Increased | No change | C57Bl/6 | 2020 | (90) |
| Mkp1 | *Mkp1*$^{-/-}$ | ♀ | 50 µg/kg/day hPTH(1-34) (5-6 days/week) | 3-24 days | Femur | ~1.250 (reported as FC) | ND | ND | C57Bl/6 129 | 2011 | (91) |
| Nf1 | *Nf1*$^{+/-}$ | ♂ | 80 µg/kg/day hPTH(1-34) | 28 days of iPTH starting 8-12 weeks | Tibia | ~0.963 | ND | Increased | C57Bl/6 | 2006 | (92) |
| Nmp4 | *Nmp4*$^{-/-}$ | ♀ | 30 µg/kg/day hPTH(1-34) | 10-17 weeks | Femur | ~2.906 | ND | ND | C57Bl/6 (6$^{th}$ generation) | 2009 | (93) |
| Nmp4 | *Nmp4*$^{-/-}$ | ♀ | 30 µg/kg/day hPTH(1-34) | 10-12 weeks | Tibia | ~1.500 | ND | ND | C57Bl/6 (6$^{th}$ generation) | 2011 | (94) |
| Nmp4 | *Nmp4*$^{-/-}$ | ♀ | 30 µg/kg/day hPTH(1-34) | 10-17 weeks | Tibia | ~0.800 | ND | ND | C57Bl/6 (6$^{th}$ generation) | 2011 | (94) |
| Nmp4 | *Nmp4*$^{-/-}$ | ♀ | 30 µg/kg/day hPTH(1-34) | 10-12 weeks | Vertebrae | ~1.467 | ND | ND | C57Bl/6 (6$^{th}$ generation) | 2011 | (94) |
| Nmp4 | *Nmp4*$^{-/-}$ | ♀ | 30 µg/kg/day hPTH(1-34) | 10-17 weeks | Vertebrae | ~4.206 | ND | ND | C57Bl/6 (6$^{th}$ generation) | 2011 | (94) |
| Nmp4 | *Nmp4*$^{-/-}$ | ♀ | 30 µg/kg/day hPTH(1-34) | 10-13 weeks | Femur | ~2.523 | ND | ND | C57Bl/6 (6$^{th}$-7$^{th}$ generation) | 2012 | (95) |
| Ocn | *Ocn*$^{-/-}$ | ♀ | 80 µg/kg/day hPTH(1-34) (5 days/week) | 10-14 weeks | Vertebrae | 1.266 | ND | ND | C57Bl/6 | 2008 | (96) |
| Ocn | *Ocn*$^{-/-}$ | ♀ | 80 µg/kg/day hPTH(1-34) (5 days/week) | 10-14 weeks | Femur | 1.174 | No change | Increased | C57Bl/6 | 2008 | (96) |
| Opn | *Opn*$^{-/-}$ | ♀ | 80 µg/kg/day hPTH(1-34) (5 days/week) | 7-11 weeks | Tibia and Femur | ~1.362** | ND | Decreased | 129 | 2003 | (97) |
| OSMR | *Osmr*$^{-/-}$ | ♂ | 30 µg/kg/day hPTH(1-34) (5 days/week) | 6-9 weeks | Tibia | ~-0.518 | Decreased | Increased | C57Bl/6 | 2011 | (98) |
| p38α | *Ocn-Cre;p38α*$^{f/f}$ | ♂ | 40 µg/kg/day hPTH(1-34) | 12-16 weeks | Femur | ~0.415 | Decreased | Decreased | C57Bl/6 | 2015 | (99) |
| Pappa | *Pappa*$^{-/-}$ | ♀ | 80 µg/kg/day hPTH(1-34) (5 days/week) | 12-18 weeks | Femur | ~0.277** | ND | ND | C57Bl/6 129 | 2015 | (100) |
| PLS3 | *Pls3*$^{-/0}$ | ♂ | 80 µg/kg/day hPTH(1-34) | 10-12 weeks | Vertebrae | ND | No change | ND | C57Bl/6 | 2020 | (101) |
| Postn | *Postn-/-* | ♀ | 40 µg/kg/day hPTH(1-34) | 12-17 weeks | Femur | 1.106 | ND | Increased | C57Bl/6 | 2012 | (102) |
| Postn | *Postn*$^{-/-}$ | ♀ | 40 µg/kg/day hPTH(1-34) | 12-17 weeks | Vertebrae | 1.762 | ND | ND | C57Bl/6 | 2012 | (102) |
| Prg4 | *Prg4*$^{-/-}$ | ♀♂ | 50 µg/kg/day hPTH(1-34) | 4-21 days | Femur | 1.239 | ND | ND | C57Bl/6 | 2012 | (20) |
| Prg4 | *Prg4*$^{-/-}$ | ♀♂ | 50 µg/kg/day hPTH(1-34) | 16-22 weeks | Femur | -9.692 | No change | Decreased | C57Bl/6 | 2012 | (20) |

FC = fold change, NI = not indicated; ND = not determined; ~ = indicates that values are estimated from a graph, **=Bone area reported

| | | | | | | | | | | | |
|---|---|---|---|---|---|---|---|---|---|---|---|
| PTH and 1α(OH)ase | *PTH$^{-/-}$;1α(OH)ase$^{-/-}$* | NI | 0.2 μg/kg/day rat PTH(1-34)/day | 4-14 days | Femur | ~62.000 | Cannot determine (no reported WT+PTH) | Cannot determine (no reported WT+PTH) | C57BL/6J and BALB/c | 2005 | (103) |
| PTH1R | *Lck-Cre;PTH1R$^{f/f}$* | ♀ | 80 μg/kg/day hPTH(1-34) | 2-6 weeks | Femur | 0.409 | Decreased | No change | C57Bl/6 | 2012 | (104) |
| PTH1R | *Lck-Cre;PTH1R$^{f/f}$* | ♀ | 80 μg/kg/day hPTH(1-34) | 13-17 weeks | Femur | -0.314 | ND | ND | C57Bl/6 | 2012 | (104) |
| PTH1R | *pdPTH1R* | ♀ | 40 μg/kg/day hPTH(1-34) (5 days/week) | 12-22 weeks | Vertebrae | ~0.837 | ND | ND | C57Bl/6 | 2012 | (105) |
| PTH1R | *pdPTH1R* | ♂ | 40 μg/kg/day hPTH(1-34) (5 days/week) | 12-22 weeks | Vertebrae | ~0.890 | ND | ND | C57Bl/6 | 2012 | (105) |
| PTH1R | *pdPTH1R* | ♀ | 40 μg/kg/day hPTH(1-34) (5 days/week) | 12-22 weeks | Femur | ~0.822 | ND | ND | C57Bl/6 | 2012 | (105) |
| PTH1R | *pdPTH1R* | ♂ | 40 μg/kg/day hPTH(1-34) (5 days/week) | 12-22 weeks | Femur | ~1.000 | ND | ND | C57Bl/6 | 2012 | (105) |
| PTH1R | *DMP1-Cre;PTH1R$^{f/f}$* | ♀ | 80 μg/kg/day hPTH(1-34) (5 days/week) | 4 weeks of iPTH (start age NI) | Femur | ND | ND | ND | C57Bl/6 dominant (mixed background) | 2013 | (106) |
| PTH1R | *DMP1-Cre;PTH1R$^{f/f}$* | ♀ | 80 μg/kg/day hPTH(1-34) (5 days/week) | 4 weeks of iPTH (start age NI) | Vertebrae | 0.339 | ND | ND | C57Bl/6 dominant (mixed background) | 2013 | (106) |
| PTH1R | *Dmp1-Cre;PTH1R$^{f/f}$* | ♀ | 100 ng/g/day PTH(1-34) | 16-20 weeks | Femur | ~0.739 | ND | ND | C57BL/6Nhsd | 2016 | (107) |
| PTH1R | *Dmp1-Cre;PTH1R$^{f/f}$* | ♂ | 100 ng/g/day PTH(1-34) | 16-20 weeks | Femur | ~-0.081 | ND | ND | C57BL/6Nhsd | 2016 | (107) |
| PTHRP | *Pthrp$^{+/-}$* | ♂ | 40 μg/kg/day hPTH(1-34) | 12-24 weeks | Femur | ~10.230 | ND | ND | FVB/N CD-1 | 2005 | (14) |
| Rac1 | *Osx-Cre;Rac1$^{-/-}$* | NI | 80 μg/kg/day hPTH(1-34) | 4-8 weeks | Femur | ND | NI | NI | NI | 2020 | (108) |
| Rac2 | *Rac2$^{-/-}$* | NI | 80 μg/kg/day hPTH(1-34) | 12-16 weeks | Tibia | ND | Increased | Increased | C57Bl/6 (used as control) | 2008 | (109) |
| Rag2 | *Rag2$^{-/-}$* | NI | 80 μg/kg/day hPTH(1-34) | 5-9 weeks | Femur | ~0.406 | ND | ND | C57Bl6/J | 2009 | (23) |
| RAGE | *RAGE$^{-/-}$* | ♀ | 30 μg/kg/day hPTH(1-34) | 10-12 weeks | Femur | ~0.00 | ND | ND | C57Bl/6 | 2010 | (110) |
| RAGE | *RAGE$^{-/-}$* | ♀ | 30 μg/kg/day hPTH(1-34) | 10-17 weeks | Femur | ~0.495 | ND | ND | C57Bl/6 | 2010 | (110) |
| RAGE | *RAGE$^{-/-}$* | ♀ | 30 μg/kg/day hPTH(1-34) | 10-12 weeks | Vertebrae | ~1.857 | ND | ND | C57Bl/6 | 2010 | (110) |
| Runx2 | *Runx2 Tg* | ♀ | 100 μg/kg/day hPTH(1-34) | 4-10 weeks | Femur | ~0.637 | ND | Increased | C57Bl/6 | 2007 | (111) |
| sFRP1 | *sFRP$^{-/-}$* | ♀ | 100 μg/kg/day hPTH(1-34) | 8-12 weeks | Femur | ~0.711 (reported as FC) | ND | ND | C57BL/6 (albino)-129SvEv (LEX-1) | 2006 | (112) |
| sFRP1 | *sFRP$^{-/-}$* | ♀ | 100 μg/kg/day hPTH(1-34) | 24-28 weeks | Femur | ~0.627 (reported as FC) | ND | ND | C57BL/6 (albino)-129SvEv (LEX-1) | 2006 | (112) |

FC = fold change, NI = not indicated; ND = not determined; ~ = indicates that values are estimated from a graph, **=Bone area reported

| | | | | | | | | | | | |
|---|---|---|---|---|---|---|---|---|---|---|---|
| sFRP1 | *sFRP*$^{-/-}$ | ♀ | 100 µg/kg/day hPTH(1-34) | 36-40 weeks | Femur | ~0.332 (reported as FC) | ND | ND | C57BL/6 (albino)-129SvEv (LEX-1) | 2006 | (112) |
| sFRP1 | *sFRP1 Tg* | ♀ | 40 µg/kg/day hPTH(1-34) (5 days/week) | 12-14 weeks | Femur | 0.103 | ND | No change | FVB/N-Swiss Webster hybrid | 2010 | (113) |
| sFRP1 | *sFRP1 Tg* | ♂ | 40 µg/kg/day hPTH(1-34) (5 days/week) | 12-14 weeks | Femur | 0.120 | ND | No change | FVB/N-Swiss Webster hybrid | 2010 | (113) |
| sFRP1 | *sFRP1 Tg* | ♀ | 40 µg/kg/day hPTH(1-34) (5 days/week) | 12-14 weeks | Vertebrae | 0.099 | ND | ND | FVB/N-Swiss Webster hybrid | 2010 | (113) |
| sFRP1 | *sFRP1 Tg* | ♂ | 40 µg/kg/day hPTH(1-34) (5 days/week) | 12-14 weeks | Vertebrae | 0.402 | ND | ND | FVB/N-Swiss Webster hybrid | 2010 | (113) |
| Sost | *Sost TG* | ♂ | 100 µg/kg/day hPTH(1-34) (5-6 days/week) | 24-33 weeks | Femur | 0.391 | ND | No change | FVB, C57BL/6 | 2010 | (114) |
| Sost | *Sost*$^{-/-}$ | ♂ | 30 µg/kg/day hPTH(1-34) | 10-16 weeks | Femur | ~0.779 | ND | ND | 129/SvJ and Black Swiss | 2011 | (115) |
| Sost | *Sost*$^{-/-}$ | ♂ | 90 µg/kg/day hPTH(1-34) | 10-16 weeks | Femur | ~0.877 | ND | ND | 129/SvJ and Black Swiss | 2011 | (115) |
| TCRβ | *TCRδ*$^{-/-}$ | NI | 80 µg/kg/day hPTH(1-34) | 5-9 weeks | Femur | 0.503 | Decreased | Increased | C57Bl/6 | 2009 | (23) |
| TGFβ1 | *TGFβ1*$^{-/-}$,*Rag2*$^{-/-}$ | ♂ | 40 µg/kg/day hPTH(1-34) (5 days/week) | 8-12 weeks | Tibia | ~-0.388 | Decreased | No change | C57Bl/6 | 2011 | (116) |
| TGIF1 | *Tgif1*$^{fl/fl}$; *DMP1-cre* | ♂ | 100 µg/kg/day hPTH(1-34) (5 days/week) | 8-12 weeks | Tibia | ~0.103 | Decreased | No change | C57Bl/6 | 2019 | (117) |
| TGIF1 | *Tgif1*$^{-/-}$ | ♂ | 100 µg/kg/day hPTH(1-34) (5 days/week) | 8-12 weeks | Tibia | ~-0.126 | Decreased | Decreased | C57Bl/6 | 2019 | (117) |
| Timp1 | *Timp1 TG by type-I collagen promoter* | ♀ | 40 µg/kg/day hPTH(1-34) | 10-16 weeks | Femur | 1.964 | ND | Decreased | C57BL/6 CBA | 2006 | (118) |
| Ts65Dn | *Mosel for trisomy 21* | ♂ | 30 µg/kg/day hPTH(1-34) | 12-16 weeks | Tibia | ~1.450 | No change | No change | C57BL/6 C3H/HeJ | 2012 | (119) |
| Ts65Dn | *Mosel for trisomy 21* | ♂ | 80 µg/kg/day hPTH(1-34) | 12-16 weeks | Tibia | ~1.450 | No change | No change | C57BL/6 C3H/HeJ | 2012 | (119) |
| Vps35 | *Ocn-Cre;Vps35*$^{f/f}$ | ♂ | 50 µg/kg/day hPTH(1-34) (5 days/week) | 7-12 weeks | Femur | ~7.690 | ND | ND | C57Bl/6 | 2016 | (120) |
| Wnt1 | *Wnt1*$^{+/R235W}$ | ♀ | 80 µg/kg/day hPTH(1-34) | 52-56 weeks | Femur | ND | ND | ND | C57Bl/6 129 | 2020 | (121) |

FC = fold change, NI = not indicated; ND = not determined; ~ = indicates that values are estimated from a graph, **=Bone area reported

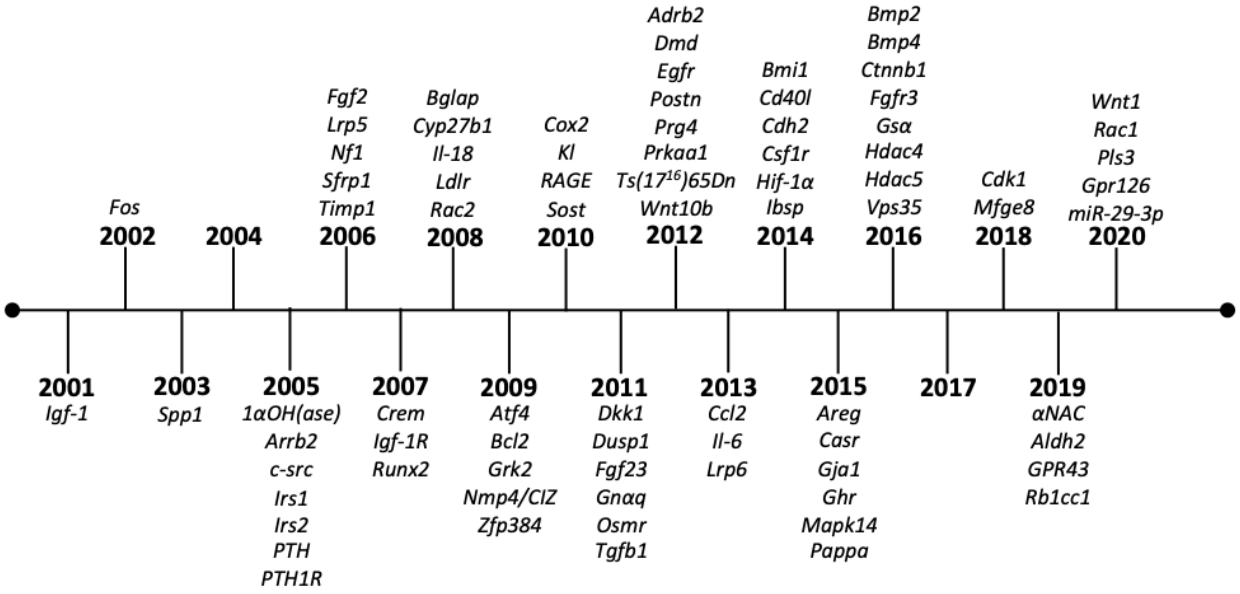


figure 1 higher res.tiff

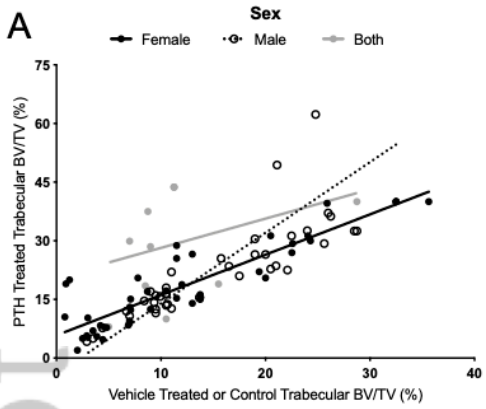


| p-value | Male | Both |
|---|---|---|
| Female | 0.0011 | 0.4584 |
| Male | | 0.1143 |

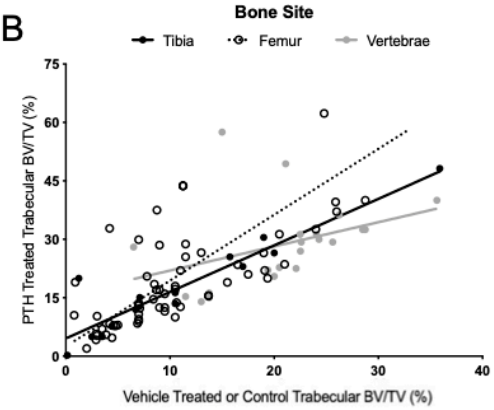


| p-value | Femur | Vertebrae |
|---|---|---|
| Tibia | 0.1756 | 0.1333 |
| Femur | | 0.0147 |

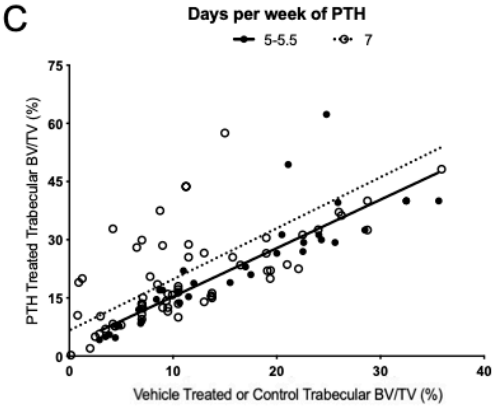


| p-value | 7 |
|---|---|
| 5-5.5 | 0.7938 |

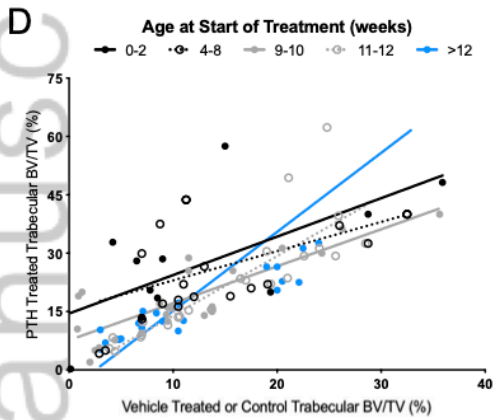


| p-value | 4-8 | 9-10 | 11-12 | >12 |
|---|---|---|---|---|
| 0-2 | 0.5765 | 0.9062 | 0.1542 | 0.0519 |
| 4-8 | | 0.4889 | 0.0212 | 0.0046 |
| 9-10 | | | 0.0226 | 0.0053 |
| 11-12 | | | | 0.2222 |

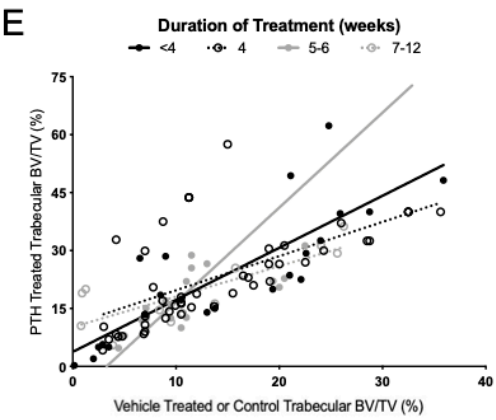


| p-value | 4 | 5-6 | 7-12 |
|---|---|---|---|
| <4 | 0.0819 | 0.0095 | 0.0898 |
| 4 | | <0.0001 | 0.7747 |
| 5-6 | | | 0.0014 |

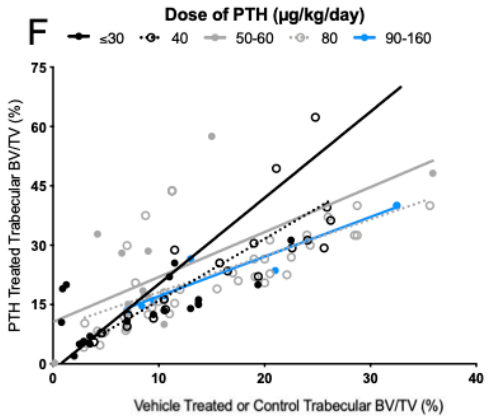


| p-value | 40 | 50-60 | 80 | 90-160 |
|---|---|---|---|---|
| ≦30 | 0.2302 | 0.1052 | 0.0009 | 0.0288 |
| 40 | | 0.3817 | 0.0389 | 0.0801 |
| 50-60 | | | 0.5649 | 0.7742 |
| 80 | | | | 0.7719 |

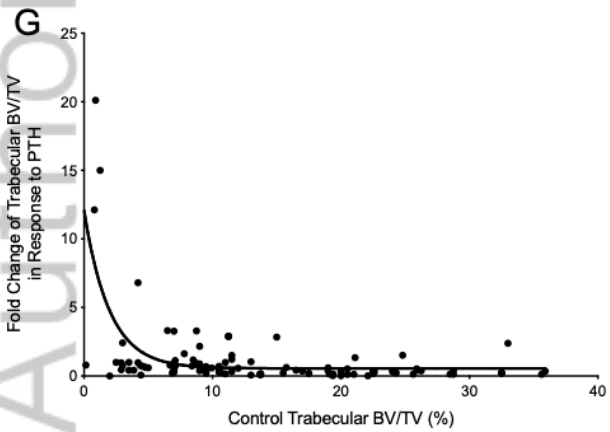




figure 2 higher res.tiff

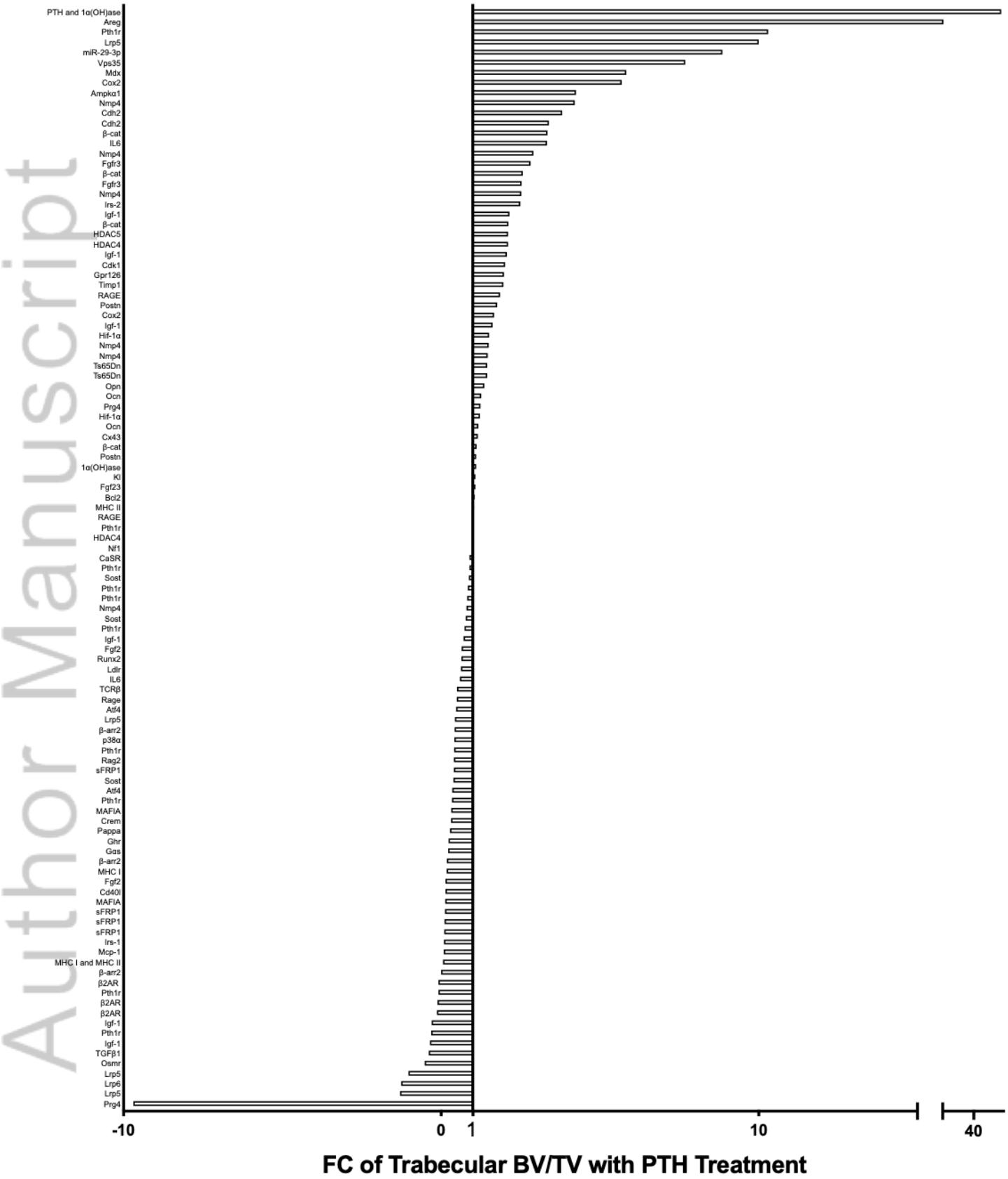




figure 3 higher res.tiff